



3 4456 0452175 6

ORNL/TM-8130

**ornl****OAK  
RIDGE  
NATIONAL  
LABORATORY****UNION  
CARBIDE****The Influence of Temperature,  
Environment, and Thermal  
Aging on the Continuous  
Cycle Fatigue Behavior  
of Hastelloy X and  
Inconel 617**

J. P. Strizak  
C. R. Brinkman  
M. K. Booker  
P. L. Rittenhouse

OAK RIDGE NATIONAL LABORATORY

CENTRAL RESEARCH LIBRARY

CIRCULATION SECTION

4500N ROOM 175

**LIBRARY LOAN COPY**

DO NOT TRANSFER TO ANOTHER PERSON

If you wish someone else to see this  
report, send in name with report and  
the library will arrange a loan.

UCN-7969 3 9-771

OPERATED BY  
UNION CARBIDE CORPORATION  
FOR THE UNITED STATES  
DEPARTMENT OF ENERGY



Printed in the United States of America. Available from  
National Technical Information Service  
U.S. Department of Commerce  
5285 Port Royal Road, Springfield, Virginia 22161  
NTIS price codes—Printed Copy: A04 Microfiche A01

This report was prepared as an account of work sponsored by an agency of the United States Government. Neither the United States Government nor any agency thereof, nor any of their employees, makes any warranty, express or implied, or assumes any legal liability or responsibility for the accuracy, completeness, or usefulness of any information, apparatus, product, or process disclosed, or represents that its use would not infringe privately owned rights. Reference herein to any specific commercial product, process, or service by trade name, trademark, manufacturer, or otherwise, does not necessarily constitute or imply its endorsement, recommendation, or favoring by the United States Government or any agency thereof. The views and opinions of authors expressed herein do not necessarily state or reflect those of the United States Government or any agency thereof.



3 4456 0452175 6

ORNL/TM-8130  
Distribution  
Category UC-77

Contract No. W-7405-eng-26

METALS AND CERAMICS DIVISION

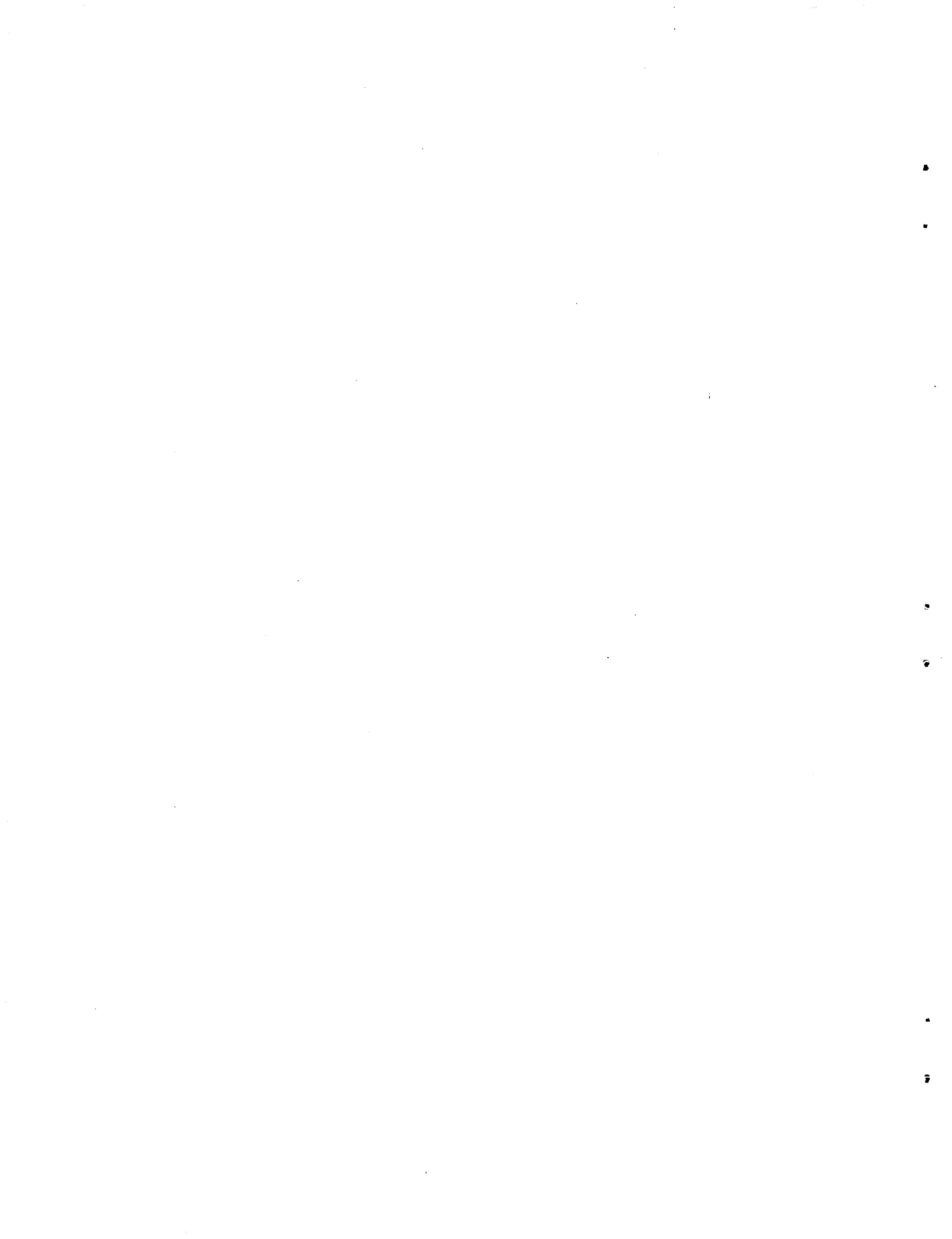
HTGR BASE TECHNOLOGY PROGRAM  
Structural Materials Program (FTP/A 01332)

THE INFLUENCE OF TEMPERATURE, ENVIRONMENT, AND THERMAL AGING  
ON THE CONTINUOUS CYCLE FATIGUE BEHAVIOR OF  
HASTELLOY X AND INCONEL 617

J. P. Strizak, C. R. Brinkman, M. K. Booker, and P. L. Rittenhouse

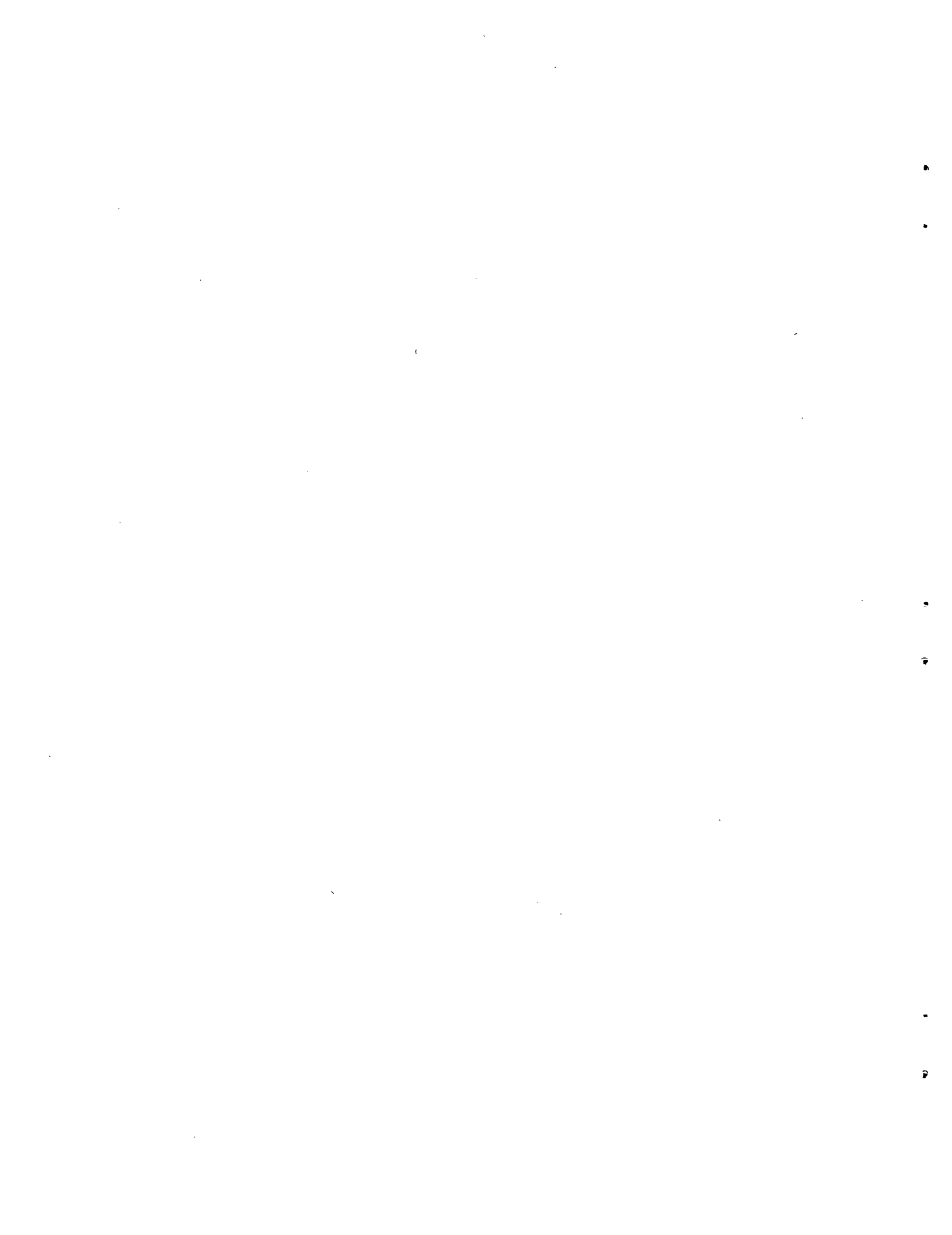
Date Published - April 1982

Prepared by  
OAK RIDGE NATIONAL LABORATORY  
Oak Ridge, Tennessee 37830  
operated by  
UNION CARBIDE CORPORATION  
for the  
DEPARTMENT OF ENERGY



## CONTENTS

ABSTRACT . . . . .	1
INTRODUCTION . . . . .	1
MATERIALS CHARACTERIZATION . . . . .	2
EXPERIMENTAL . . . . .	3
RESULTS AND DISCUSSION . . . . .	4
CONCLUSIONS . . . . .	13
ACKNOWLEDGMENTS . . . . .	14
REFERENCES . . . . .	14
APPENDIX A — MICROSTRUCTURES OF TWO TEST MATERIALS . . . . .	15
APPENDIX B — FATIGUE DATA . . . . .	29
APPENDIX C — PROPOSED FATIGUE DESIGN CURVES . . . . .	41



THE INFLUENCE OF TEMPERATURE, ENVIRONMENT, AND THERMAL AGING  
ON THE CONTINUOUS CYCLE FATIGUE BEHAVIOR OF  
HASTELLOY X AND INCONEL 617

J. P. Strizak, C. R. Brinkman, M. K. Booker, and P. L. Rittenhouse

ABSTRACT

We present results of strain-controlled fatigue and tensile tests for two nickel-base, solution-hardened reference structural alloys for use in several High-Temperature Gas-Cooled Reactor (HTGR) concepts. These alloys, Hastelloy X and Inconel 617, were tested from room temperature to 871°C in air and impure helium. Materials were tested in both the solution-annealed and the preaged conditions, in which aging consisted of isothermal exposure at one of several temperatures for periods of up to 20,000 h. Comparisons are given between the strain-controlled fatigue lives of these and several other commonly used alloys, all tested at 538°C. An analysis is also presented of the continuous cycle fatigue data obtained from room temperature to 427°C for Hastelloy G, Hastelloy X, Hastelloy C-276, and Hastelloy C-4, an effort undertaken in support of ASME code development.

---

INTRODUCTION

Hastelloy X and Inconel 617, both solid-solution-strengthened nickel-base alloys, are currently reference materials for fabrication of a number of high-temperature components of High-Temperature Gas-Cooled Reactor (HTGR) steam cycle-cogeneration and reformer systems. The first of these alloys, Hastelloy X, has been used successfully for almost three decades in a variety of elevated-temperature applications requiring high strength. Its most extensive use in the HTGR is expected to be as a thermal barrier cover plate material. Industrial experience with the second alloy, Inconel 617, is much more limited, but this alloy has the distinction of possessing high creep resistance at elevated temperatures. It is therefore considered to be the leading candidate for construction of the intermediate heat exchanger for the reformer system.

The HTGR applications anticipated for these alloys require that low- and high-cycle fatigue data be available to satisfy the demands of engineering design data, codes (as in Sect. T-1400 of ASME Code Case N-47-17), and licensing. In addition to the basic low-cycle fatigue data, information is needed on the effects of service life and environment particularly because carburization may be expected at elevated temperatures in HTGR primary coolant helium. To satisfy these needs, a program of low-cycle fatigue testing was undertaken on Hastelloy X and Inconel 617. The baseline data were determined on solution-annealed (unaged) materials. Specimens aged for up to 20,000 h at anticipated service temperatures were then tested for comparison. Both air and HTGR helium were used as test environments.

#### MATERIALS CHARACTERIZATION

The materials used in this study are characterized in Table 1. Hourglass-shaped gage section fatigue specimens were fabricated from

Table 1. Characterization of 12.7-mm-plate  
(1/2-in.) alloy<sup>a</sup>

	Inconel 617	Hastelloy X
Heat	XX01A3U5	2600-3-4936
Content, wt %		
Ni	57.35	Balance
Cr	20.30	21.82
Co	11.72	1.68
Mo	8.58	9.42
Fe	1.01	19.09
Al	0.76	
Si	0.16	0.44
C	0.07	0.07
Mn	0.05	0.58
S	0.004	<0.005
W		0.63
Source	INCO <sup>b</sup>	Cabot
Grain size	31.0 (ASTM 2)	7.8 (ASTM 4)

<sup>a</sup>Heat treatment: solution-annealed at 1177°C followed by a rapid cool.

<sup>b</sup>International Nickel Co.

blanks cut from the plate materials characterized in Table 1. The gage diameter of the resultant specimens was 5.08 mm with a radius-to-diameter ratio (R/D) of 6. The surface finish of the gage section was 0.20 to 0.28  $\mu\text{m}$ . Tensile test specimens were fabricated to 6.35-mm diameter and 31.8-mm gage length. In addition to fabricating specimens in the solution-annealed condition, specimens were also fabricated from blanks aged in an argon environment for periods of either 10,000 or 20,000 h at 538, 704, or 871°C.

Details of the alloy microstructures as a function of aging time and temperature are given in Appendix A. Also included are hardness and grain size measurements taken from the blanks subsequent to aging. Changes in the microstructure (precipitation) of Hastelloy X (Figs. A.1 through A.4) were apparent after exposure of 20,000 h at 538°C and extensive after 10,000 h at 871°C (Figs. A.6 through A.12). In the Inconel 617, a fine precipitate was apparent after exposure of about 10,000 h at 704°C (Fig. A.9), with some growth and agglomeration occurring after 10,000 h at 871°C (Fig. A.11). The hardness values in Appendix A showed increases for Hastelloy X exposed in excess of 10,000 h at 871°C. Hardness changes in Inconel 617 were found to occur, with increases apparent after exposure of 10,000 h at 538°C and with overaging and resultant decreases occurring after 10,000 h at 871°C.

All specimens for fatigue and tensile tests were taken with the specimen major axis parallel to the plate rolling direction.

#### EXPERIMENTAL

Strain-controlled fully reversed fatigue tests were conducted from room temperature to 871°C and at a cyclic strain rate of  $4 \times 10^{-3}/\text{s}$  unless stated otherwise. Desired temperatures were achieved by induction heating. Fatigue tests were conducted in air and in a typical service environment for gas-cooled reactors, which is impure helium. The composition of the gas was 30.39 Pa (300  $\mu\text{atm}$ )  $\text{H}_2$ , 3.04 Pa (30  $\mu\text{atm}$ )  $\text{CH}_4$ , 2.02 Pa (20  $\mu\text{atm}$ )  $\text{CO}$ , and 0.20 Pa (2  $\mu\text{atm}$ )  $\text{H}_2\text{O}$ , and the gas pressure in the environmental chamber was 83 kPa gage (1.8 atm). Additional details on experimental equipment used in the fatigue tests have been published.<sup>1</sup>

Tensile tests were conducted at a 0.004/min nominal strain rate [2.17  $\mu\text{m/s}$  (0.005 in./min) crosshead speed] from room temperature to 871°C.

Continuous cycle fatigue data generated under this program are presented in Appendix B, Table B.5.

## RESULTS AND DISCUSSION

The tensile properties for these two alloys are compared in Fig. 1. It is apparent for the indicated heats that these materials have similar tensile properties in the solution-annealed condition. Hastelloy X showed a characteristic ductility<sup>2</sup> minimum from about 500 to 750°C in both the solution-annealed and aged conditions. Thermal aging did not significantly change the ultimate tensile strength of Hastelloy X in the temperature range studied, but there was some indication that aging for periods of about 2500 h at 700°C increased the yield strength and ductilities. However, continued aging tended to restore these properties to the original solution-annealed values. For Inconel 617 there was a slight increase in tensile strength with aging time, particularly at 700 and 871°C. Yield strengths increased at 538 and 700°C with increasing aging times, but ductilities dropped slightly.

Figure 2 is a summary plot of all known U.S. load- and strain-controlled fully reversed fatigue data generated in air and available at room temperature for Hastelloy X.<sup>1,3,4</sup> These data, along with other Hastelloy X data generated at 427°C, were combined with test data generated on other Hastelloy alloys in order to formulate fatigue curves to be submitted to the American Society for Mechanical Engineers (ASME) Code Group for consideration in fatigue design in Sections III and VIII of the code (see Appendix C). In curve-fitting the strain-controlled data in Fig. 2, load-controlled data were omitted from the analysis if the specimen did not fail or if failure occurred at cycle lives of less than  $10^6$ . Hastelloy X is a cyclic-hardening material, and it was felt that load-controlled data with cycle lives of less than about  $10^6$  were influenced by a variable range in plasticity and were therefore not equivalent to the strain-controlled data. These data show behavior similar to that of stainless steels.<sup>5</sup>

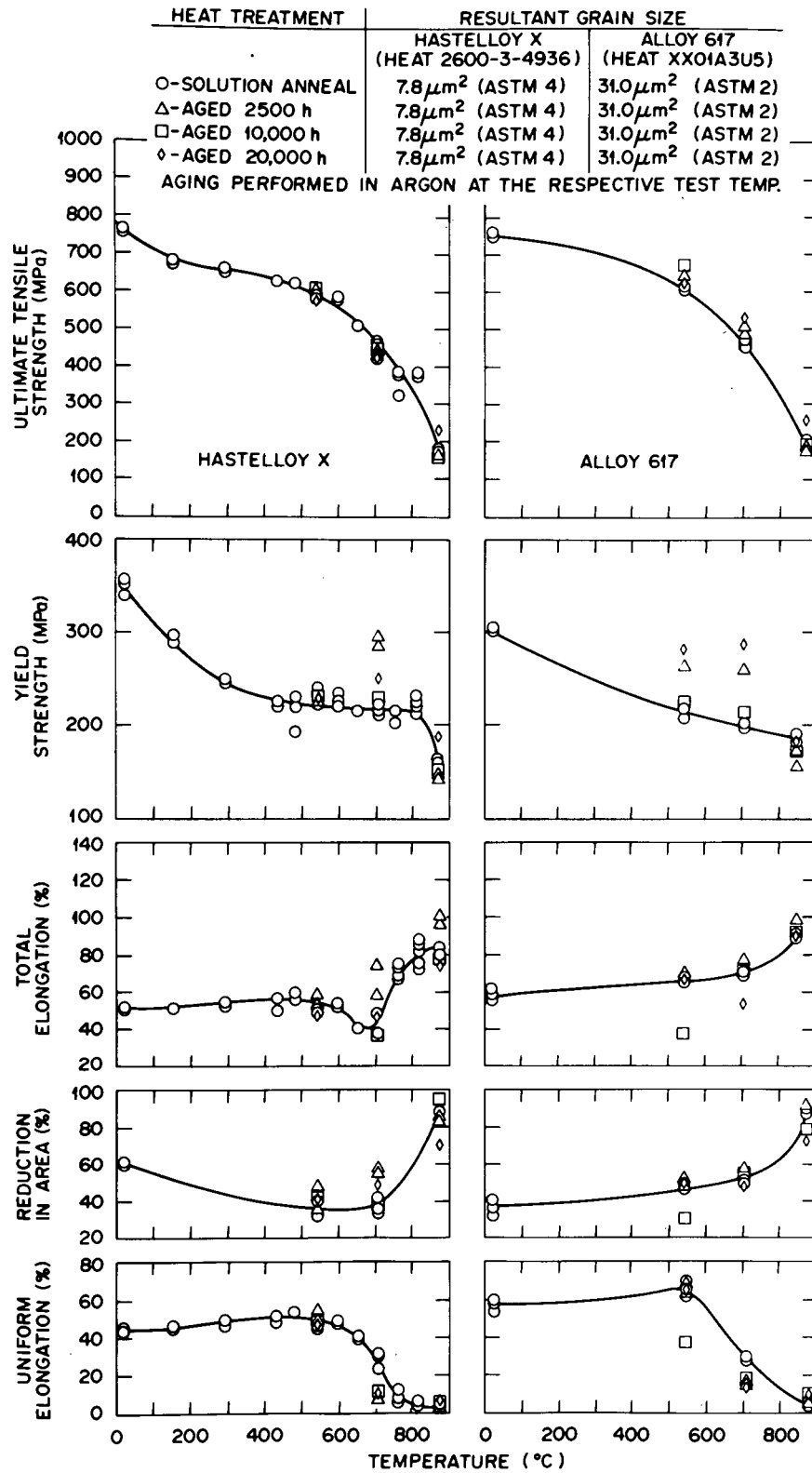


Fig. 1. Comparison of tensile properties of Hastelloy X and Inconel 617 in both solution-annealed and aged conditions.

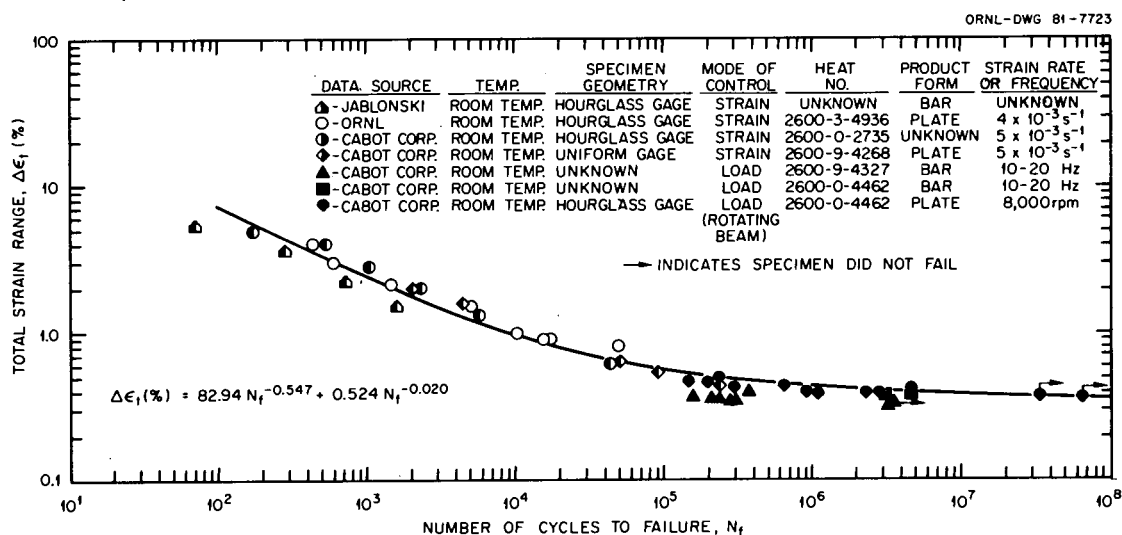


Fig. 2. Comparison of data obtained from several heats, product forms, and test techniques at room temperature for Hastelloy X. Only load-control data from tests that failed in excess of  $1 \times 10^6$  cycles were used in curve-fitting.

Figure 3 contains additional strain-controlled data for Hastelloy X generated at several temperatures in air to  $871^\circ\text{C}$ . Data shown were generated at ORNL<sup>1</sup> and by Jaske.<sup>6</sup> A significant decrease in continuous cycle fatigue life is apparent between room temperature and  $538^\circ\text{C}$ .

Figures 4 and 5 compare data generated from Hastelloy X specimens in the solution-annealed or solution-annealed-plus-aged conditions, in which the aging and test temperature were identical. Data plotted in Fig. 4 were generated at  $538^\circ\text{C}$  in either an air or an impure helium environment. Little (beneficial) or no effect of the helium environment is seen on resultant fatigue life compared with data obtained in air, but thermal aging before testing can reduce fatigue life, depending on the prior exposure time. Figure 5 shows that a thermal aging treatment for 10,000 h decreases the resultant low-cycle life when the material aging and test temperature are at  $871^\circ\text{C}$  but that cycle life is restored when the thermal aging time is extended to 20,000 h. These changes are probably due to subtle changes in the microstructure and resultant changes in ductility. Most of the data given in Figs. 3 through 5 were fit as the sum of two

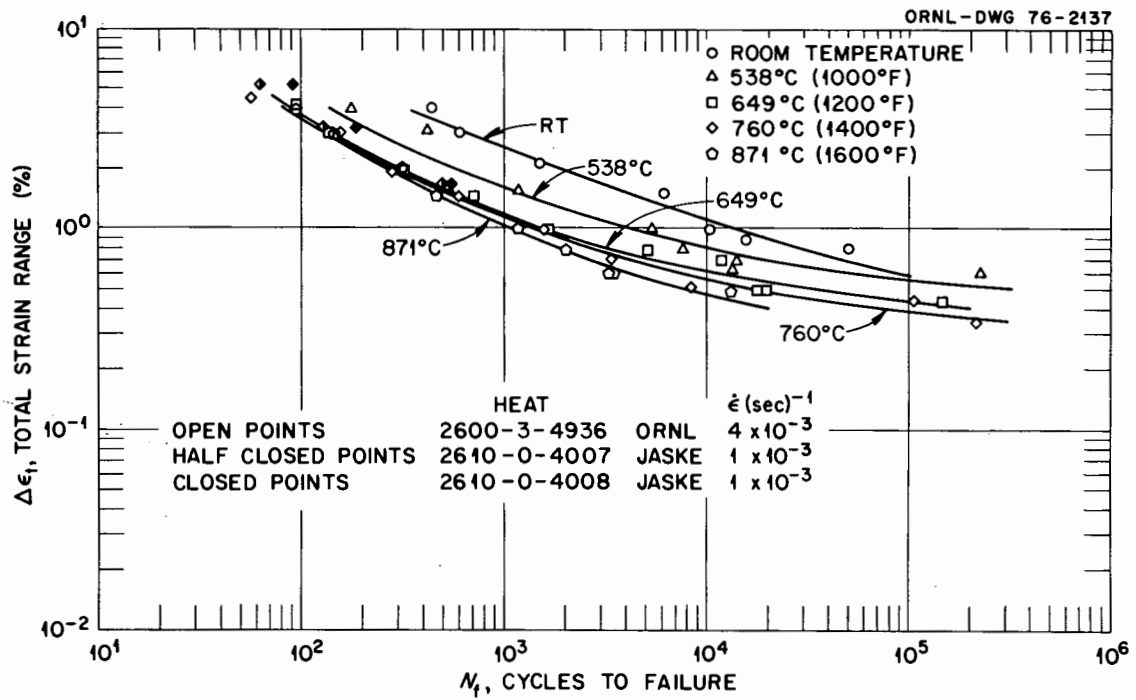


Fig. 3. Total strain range versus cycles to failure for Hastelloy X tested in air.

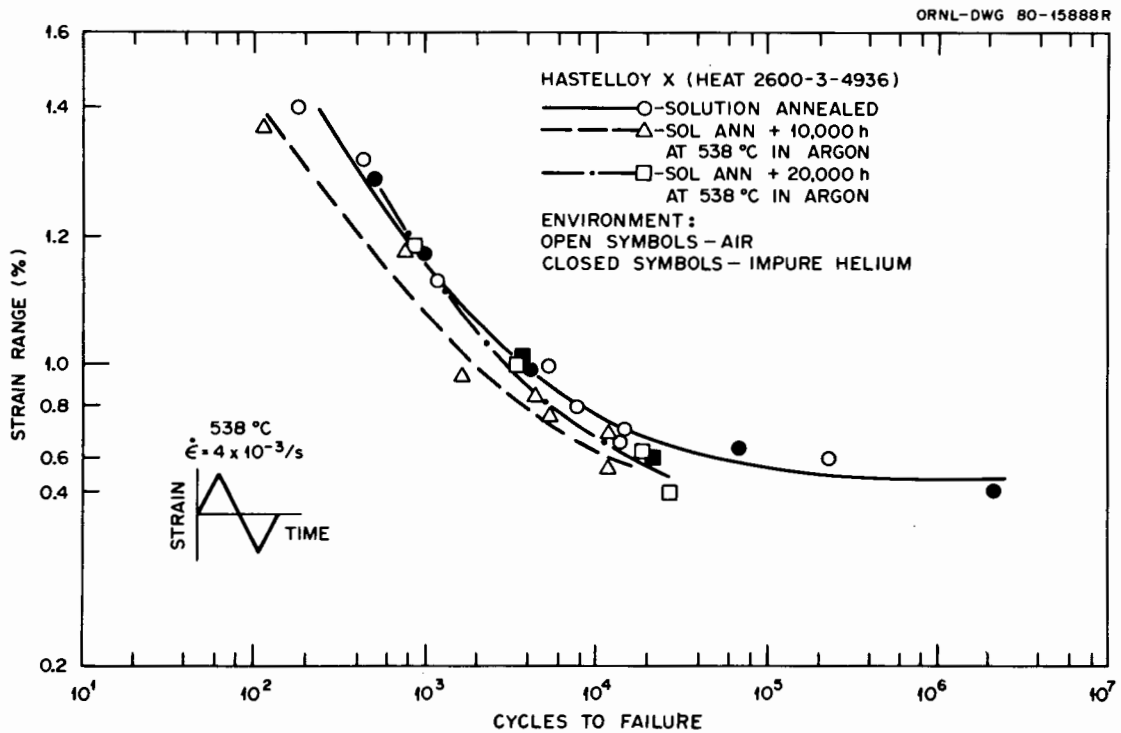


Fig. 4. Comparison of strain-controlled fatigue data generated at 538°C in air and impure helium for Hastelloy X in several conditions.

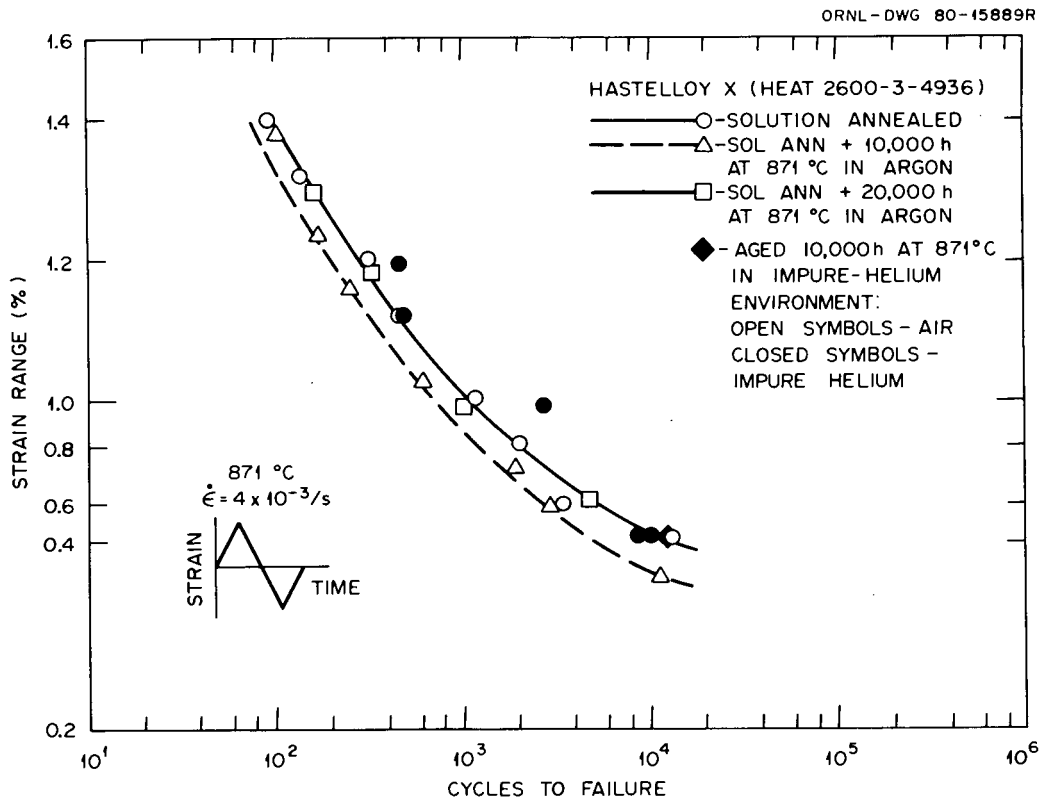


Fig. 5. Comparison of strain-controlled fatigue data generated at 871°C in air and impure helium for Hastelloy X in several conditions.

simple power law terms for the elastic and plastic components of the total strain range. The results of this analysis are given in Table 2 for Hastelloy X.

Results of similar tests conducted on Inconel 617 are plotted in Figs. 6 through 8 with power law fit constants given in Table 3 for data generated at 538, 704, and 871°C. The results obtained to date on the effects of thermal aging indicate a mixed response. At 538°C there appears to be a clear trend that long-term thermal aging results in improved cycle life with increasing time. Aging for 10,000 h before testing at 704°C appears to reduce fatigue life somewhat at this temperature (Fig. 7), but aging for 20,000 h at this temperature improved fatigue life slightly. Similar trends were noted in the data generated at 871°C (Fig. 8). These changes were attributed to microstructural changes

Table 2. Values of constants and exponents describing the best-fit fatigue curves<sup>a</sup> for Hastelloy X (heat 2600-3-4936)

Temperature (°C)	$\Delta\epsilon_t = AN_f^{-\alpha} + BN_f^{-b}, \%$			
	A	$\alpha$	B	b
Solution-annealed material				
22	56.8	0.489	1.607	0.126
538	201.3	0.753	1.288	0.093
649	87.7	0.730	1.191	0.089
704	50.4	0.623	0.736	0.064
871	67.2	0.657	0.537	0.065
Material aged 10,000 h <sup>b</sup>				
538	56.3	0.642	1.288	0.093
871	60.8	0.682	0.929	0.125
Material aged 20,000 h <sup>b</sup>				
538	192.3	0.761	1.288	0.093
871	53.1	0.627	0.929	0.125

<sup>a</sup>Strain-controlled fatigue testing at a strain rate of  $4 \times 10^{-3}$ /s.

<sup>b</sup>Aged in argon at the respective test temperature.

noted in posttest examination of the specimens. Results of testing Inconel 617 in impure helium (Fig. 8) indicated an improved cycle life in the helium environment.

Comparing the data generated in impure helium with those generated in air (Figs. 4 through 8) shows that the helium environment was in no case detrimental to fatigue life for these alloys but was, in fact, usually beneficial.

Finally, Fig. 9 compares the strain-controlled fatigue lives at 538°C of these two alloys in the solution-annealed condition with those of other commonly used structural alloys. Differences become particularly apparent in the high cycle-region. Hastelloy X also had a higher fatigue resistance than Inconel 617 when both were compared in the solution-annealed condition. Figure 10 compares cyclic stress strain curves for these alloys based on  $N_f/2$  values of stress. Little or no difference was apparent between these two alloys, and no effect of thermal aging was noted.

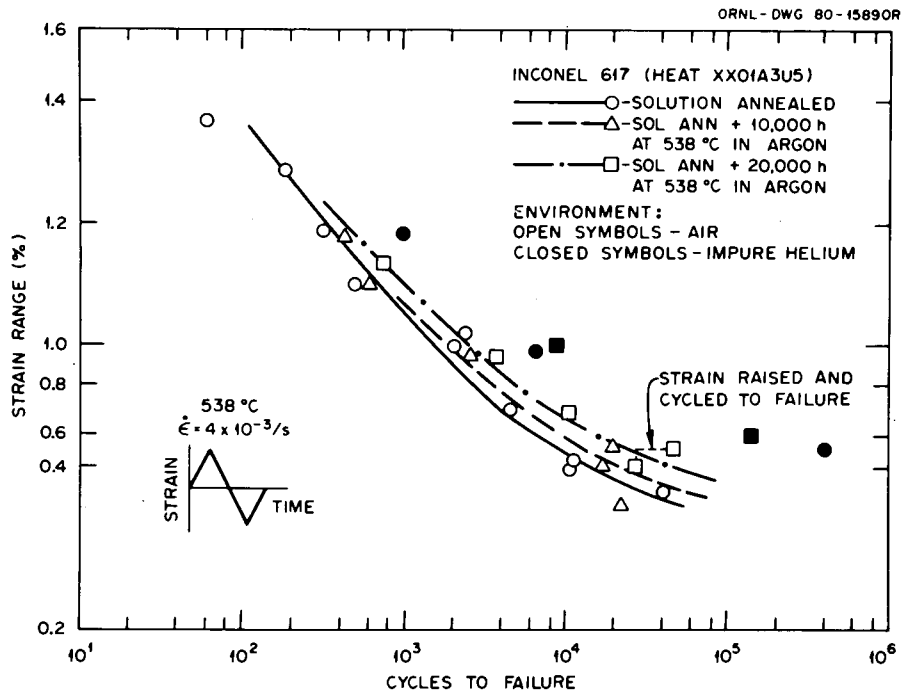


Fig. 6. Comparison of low-cycle fatigue behavior of Inconel 617 tested in air and impure helium at 538°C.

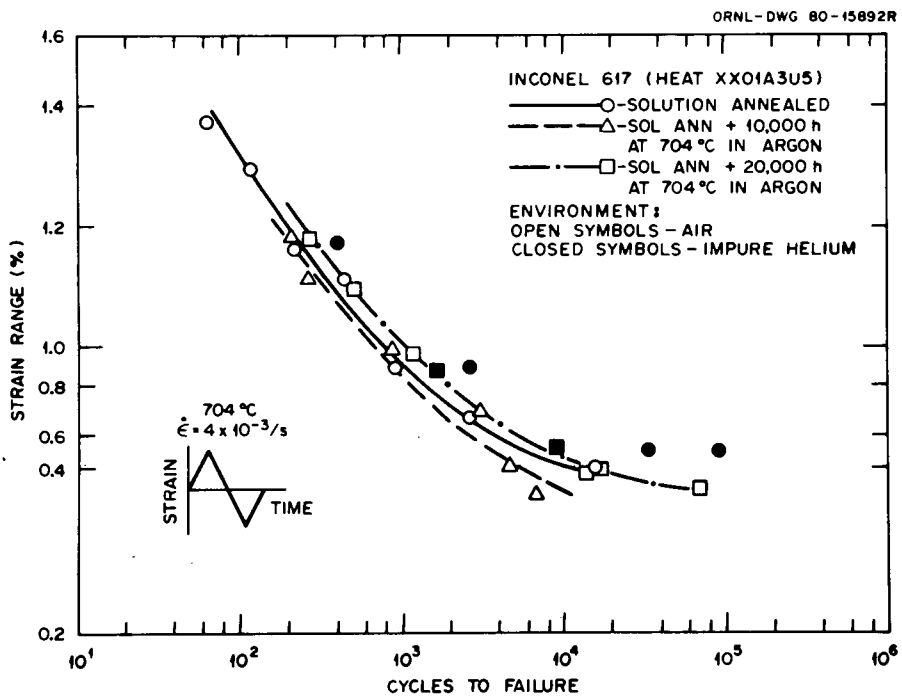


Fig. 7. Comparison of low-cycle fatigue behavior of Inconel 617 tested in air and impure helium at 704°C.

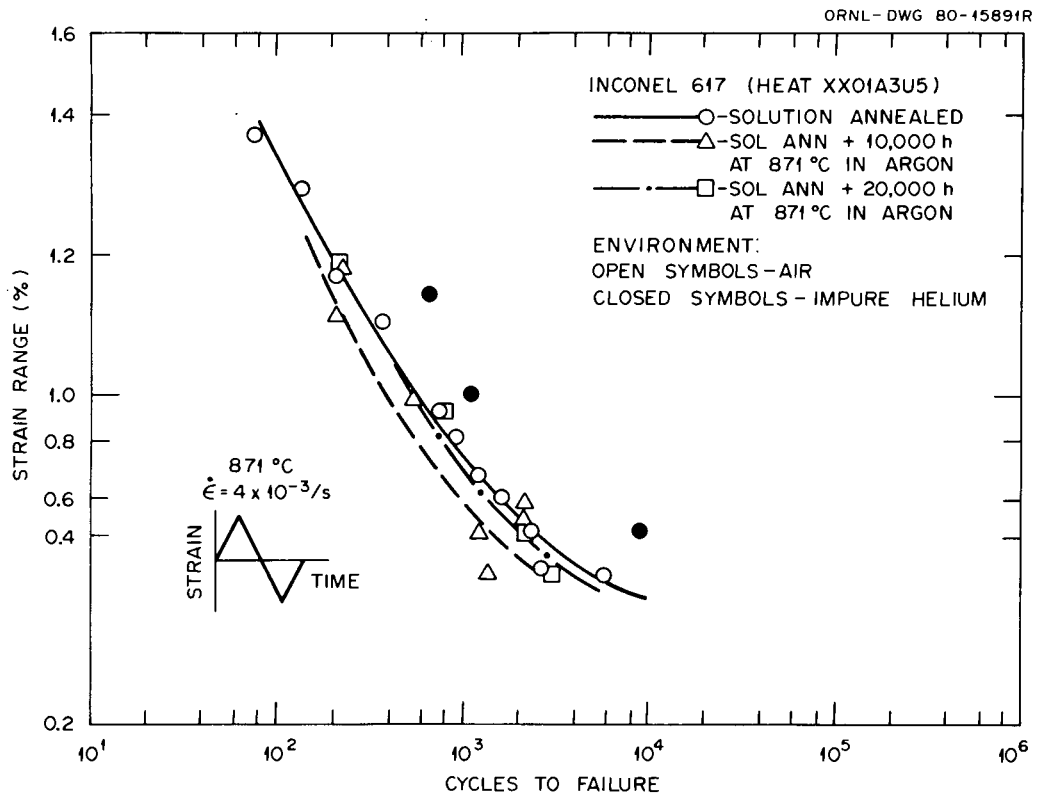


Fig. 8. Comparison of low-cycle fatigue behavior of Inconel 617 tested in air and impure helium at 871°C.

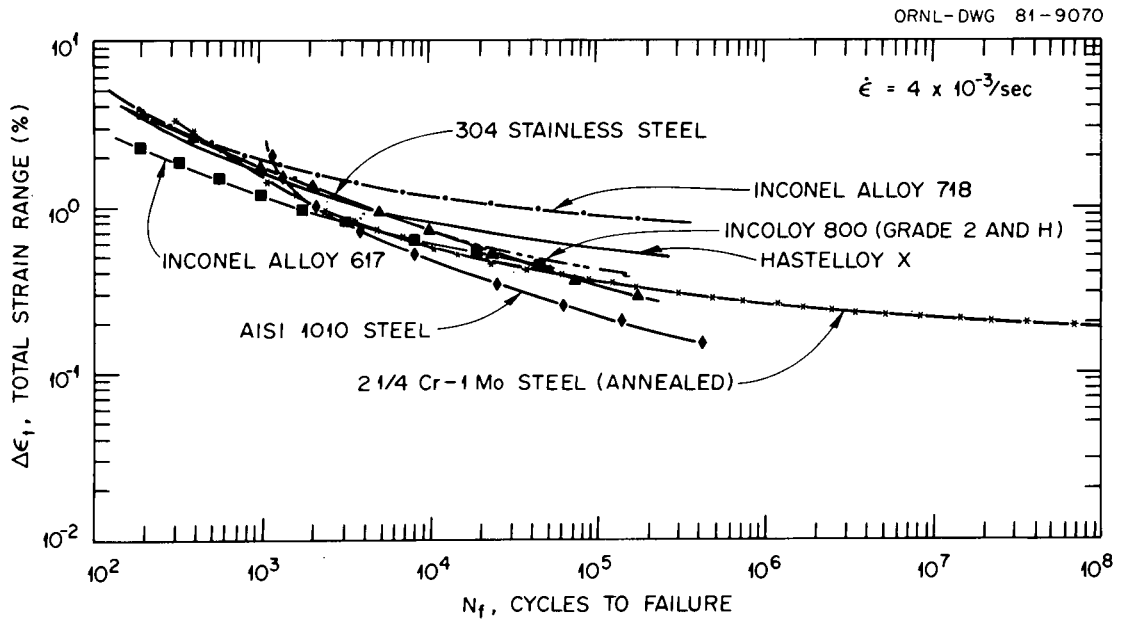


Fig. 9. Comparison of fatigue behavior of several materials at 538°C. Lines represent best-fit values of actual data. Data for type 304 stainless steel include tests at 538 and 566°C.

Table 3. Values of constants and exponents describing the best-fit fatigue curves<sup>a</sup> for Inconel 617 (heat XXX01A3U5)

Temperature (°C)	$\Delta\epsilon_t = AN_f^{-a} + BN_f^{-b}, \%$			
	A	a	B	b
Solution-annealed material				
538	67.9	0.687	1.530	0.127
704	70.8	0.738	1.379	0.121
871	128.0	0.843	0.953	0.138
Material aged 10,000 h <sup>b</sup>				
538	38.2	0.606	1.530	0.127
704	70.3	0.774	1.379	0.121
871	218.1	0.983	0.953	0.138
Material aged 20,000 h <sup>b</sup>				
538	106.9	0.693	1.530	0.127
704	72.7	0.792	1.379	0.121
871	245.9	0.941	0.953	0.138

<sup>a</sup>Strain-controlled fatigue testing at a strain rate of  $4 \times 10^{-3}$ /s.

<sup>b</sup>Aged in argon at the respective test temperature.

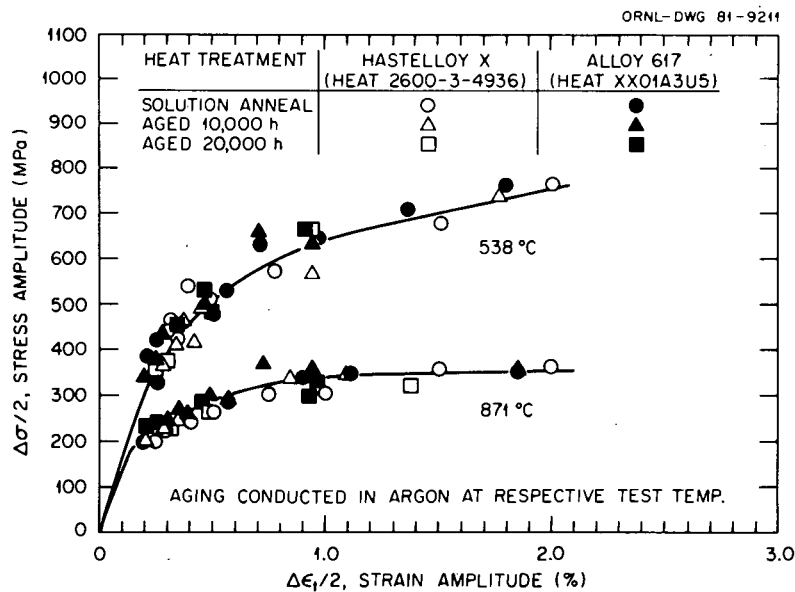


Fig. 10. Cyclic stress-strain curves for Hastelloy X and Inconel 617.

## CONCLUSIONS

A comparison was made of available strain-controlled fatigue data of Hastelloy X and Inconel 617 from room temperature to 871°C. Results included continuous cycling data obtained both in air and in an impure helium environment. Data were presented that had been generated on these alloys in the solution-annealed and in the solution-annealed and aged conditions. Preaging of the alloys occurred up to 20,000 h. We concluded

1. Thermal aging did not significantly alter the ultimate tensile strength of Hastelloy X; however, we observed some indication of changes in the yield strength and ductility properties, depending on aging time and temperature. Thermal aging increased the tensile and yield strengths of Inconel 617 somewhat, but ductilities decreased slightly again, depending on aging conditions.

2. Low- and high-cycle fatigue properties of Hastelloy X generated at room temperature were similar to those of the austenitic stainless steels. However, as the temperature increased, differences became apparent, particularly at the high-cycle end of the curves, with Hastelloy X showing the superior resistance to isothermal fatigue.

3. Prior thermal aging of Hastelloy X at either 538 or 871°C reduced fatigue life slightly, depending on the aging time. Testing of this alloy in an impure helium environment resulted in no significant differences and in some instances more low-cycle fatigue resistance.

4. The influence of prior thermal aging on the elevated-temperature low-cycle fatigue behavior of Inconel 617 was dependent on time and temperature, and both small increases and decreases were found in subsequent fatigue life. An impure helium environment was generally beneficial or resulted in little or no change in fatigue resistance of this alloy.

5. Hastelloy X shows low-cycle fatigue properties superior to those of Inconel 617 when tested at elevated temperatures (538°C) in an air environment.

6. Fatigue data for Hastelloy X, G, C-276, and C-4 from room temperature to 427°C were combined into a single data population for analysis and development of fatigue design curves for Section III of the ASME Code.

## ACKNOWLEDGMENTS

The authors gratefully acknowledge the assistance of L. K. Egner and B. McNabb, Jr., for conducting the tests. Credit is also due to K. C. Liu and M. K. Booker for reviewing the manuscript. Finally, the authors wish to thank Fauna Stooksbury for typing the draft, Irene Brogden for editing, and P. T. Thornton for preparing the final manuscript.

## REFERENCES

1. C. R. Brinkman et al., *Application of Hastelloy X in Gas-Cooled Reactor Systems*, ORNL/TM-5405, October 1976.
2. M. A. Arkoosh and N. F. Fiore, "Elevated Temperature Ductility Minimum in Hastelloy Alloy X," *Metall. Trans.* 3: 2235-40 (1972).
3. D. A. Jablonski, "Fatigue Behavior of HASTELLOY X at Elevated Temperature in Air, Vacuum, and Oxygen Environments," Ph.D. thesis, Massachusetts Institute of Technology, Cambridge, February 1978.
4. A. Aizaz, Cabot Corporation, Kokomo, Indiana, personal communication to C. R. Brinkman, March 1981.
5. B. F. Langer, "Design of Pressure Vessels for Low-Cycle Fatigue," *Trans. ASME*, 84(3): 389-402 (1962).
6. C. E. Jaske and T. L. Portilio, *Low-Cycle Fatigue of Type 347 Stainless Steel and Hastelloy Alloy X in Hydrogen Gas Environment*, TID/SNA 2047, Battelle Columbus Laboratories, Columbus, Ohio, 1971.

## Appendix A

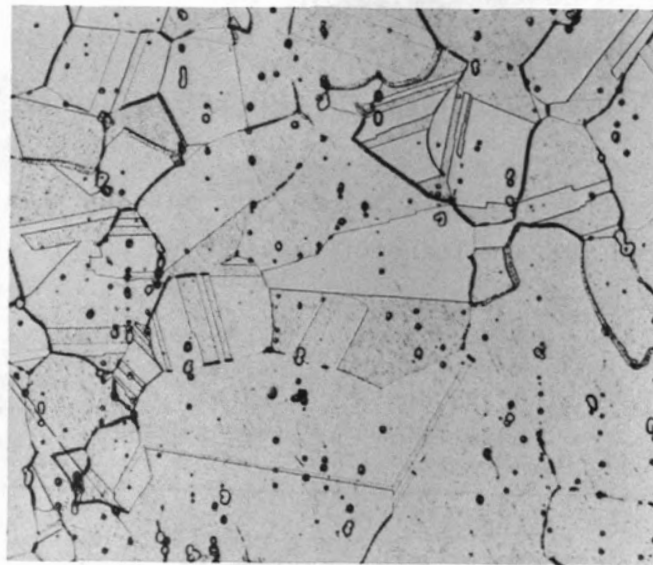
## MICROSTRUCTURES OF TWO TEST MATERIALS

Photomicrographs, hardness values, and results of grain size measurements are reported for specimens of Hastelloy X and Inconel 617 aged as shown in Table A.1.

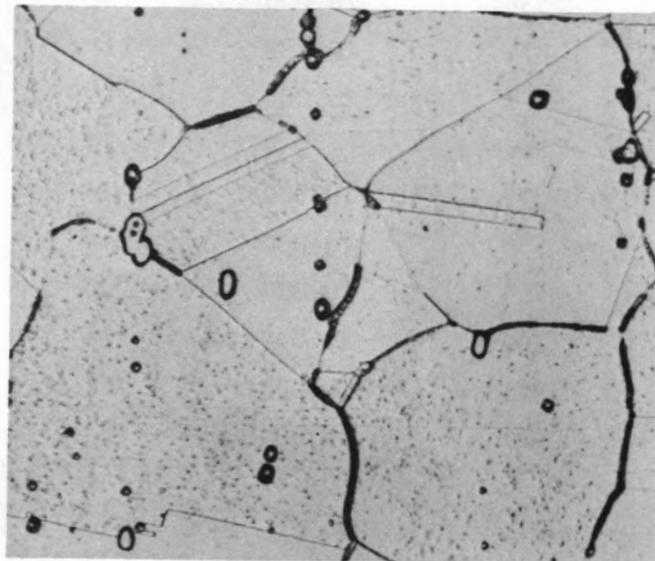
Table A.1. Aging, hardness, and grain sizes of Hastelloy X and Inconel 617 specimens

Material	Aging temperatures (°C)	Aging time (h)	Hardness (DPH)	Approximate grain size (ASTM)
Hastelloy X	None	0	183	4
Hastelloy X	538	10,000	188	4
Hastelloy X	538	20,000	182	4
Hastelloy X	871	10,000	211	4
Hastelloy X	871	20,000	218	4
Inconel 617	None	0	172	2
Inconel 617	538	10,000	208	2
Inconel 617	538	20,000	204	2
Inconel 617	704	10,000	205	2
Inconel 617	704	20,000	226	2
Inconel 617	871	10,000	175	2
Inconel 617	871	20,000	183	2

ORNL-Photo 5583-81



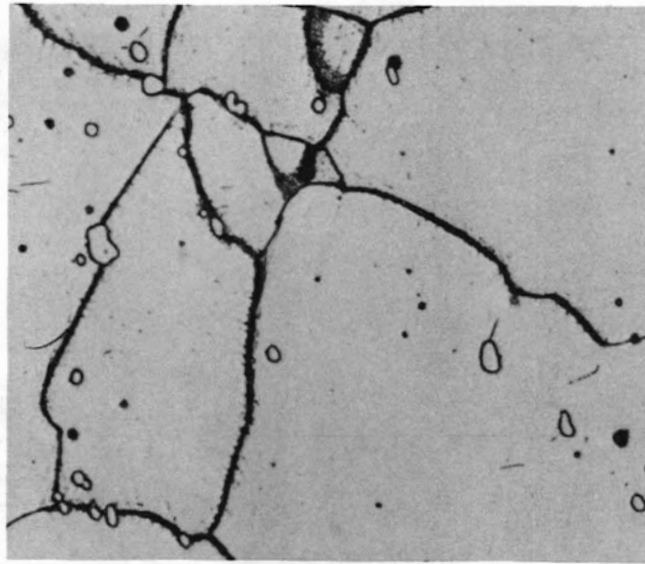
(a)

40  $\mu\text{m}$ 

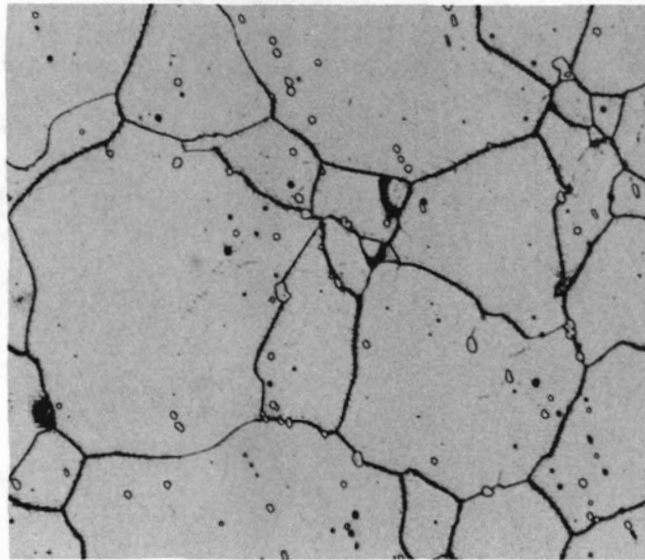
(b)

100  $\mu\text{m}$ 

Fig. A.1. Hastelloy X in solution-annealed condition.



(a)

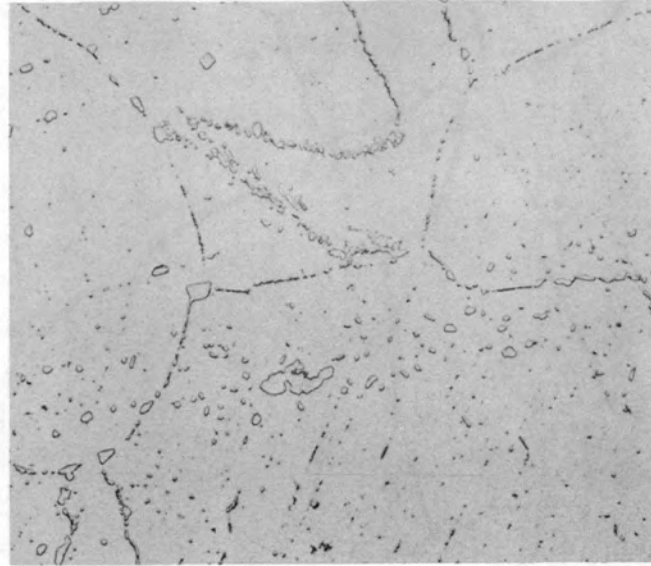
40  $\mu\text{m}$ 

(b)

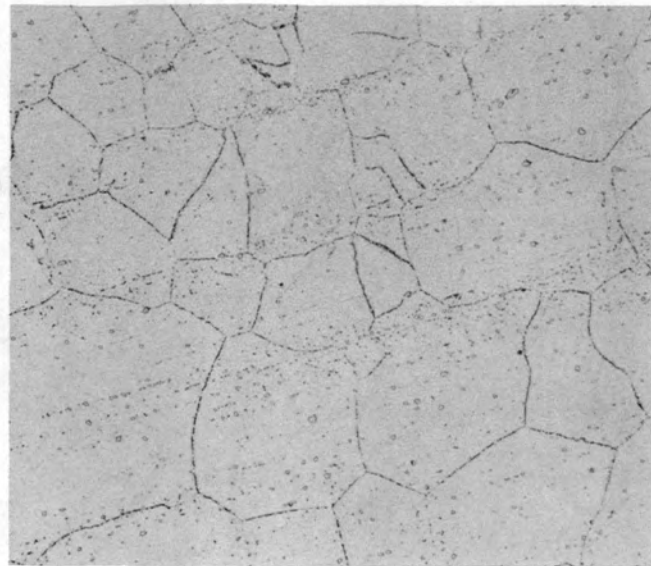
100  $\mu\text{m}$ 

Fig. A.2. Hastelloy X aged 10,000 h at 538°C.

ORNL-Photo 5585-81



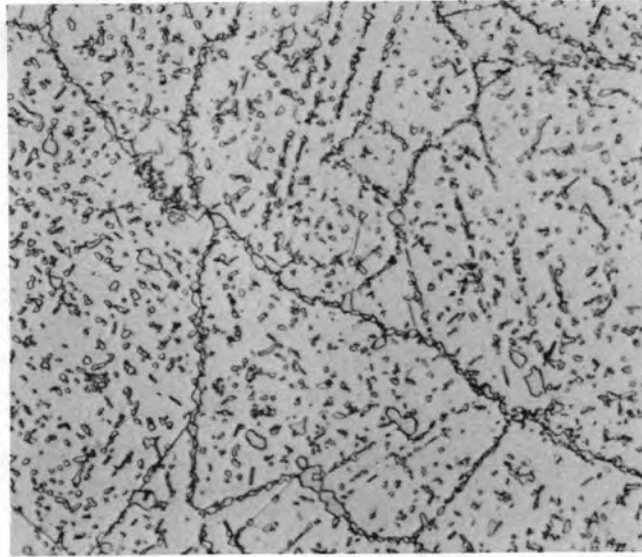
(a)

40  $\mu\text{m}$ 

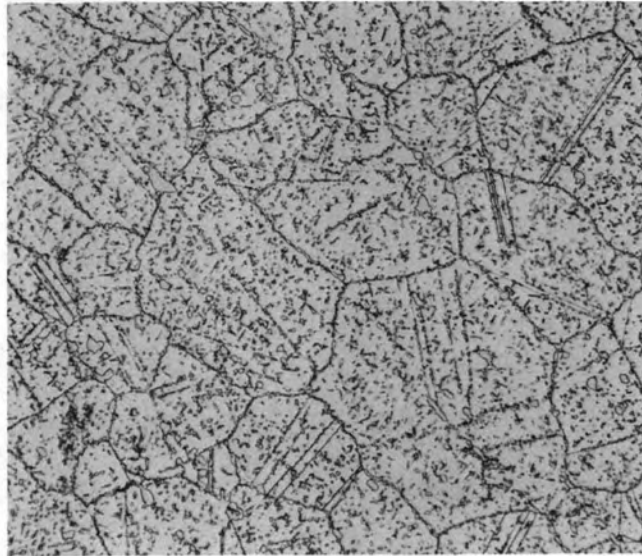
(b)

200  $\mu\text{m}$ 

Fig. A.3. Hastelloy X aged 20,000 h at 538°C.



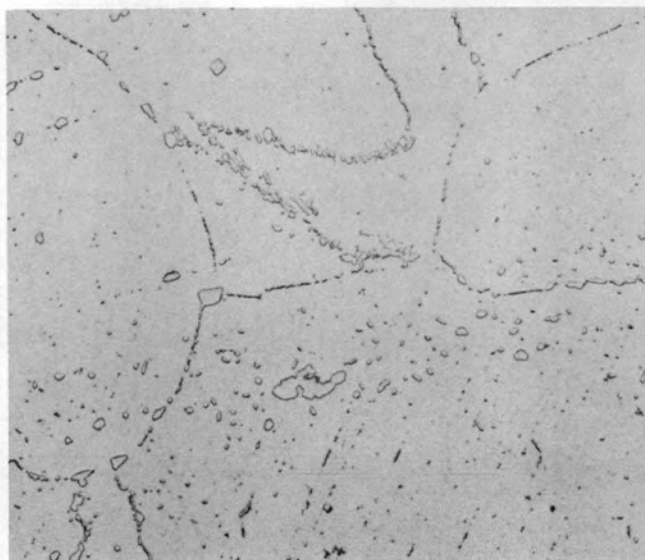
(a)

40  $\mu\text{m}$ 

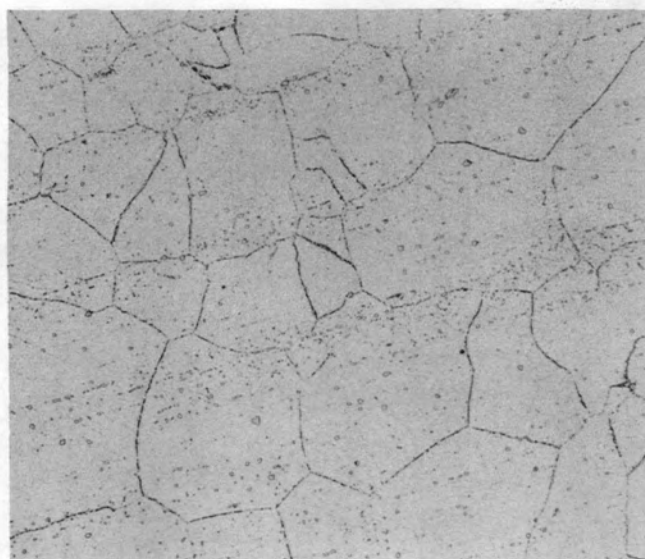
(b)

100  $\mu\text{m}$ 

Fig. A.4. Hastelloy X aged 10,000 h at 871°C.



(a)

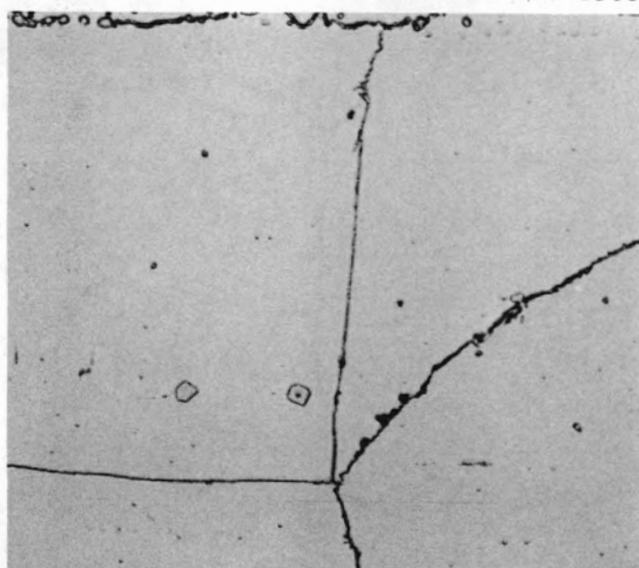
40  $\mu\text{m}$ 

(b)

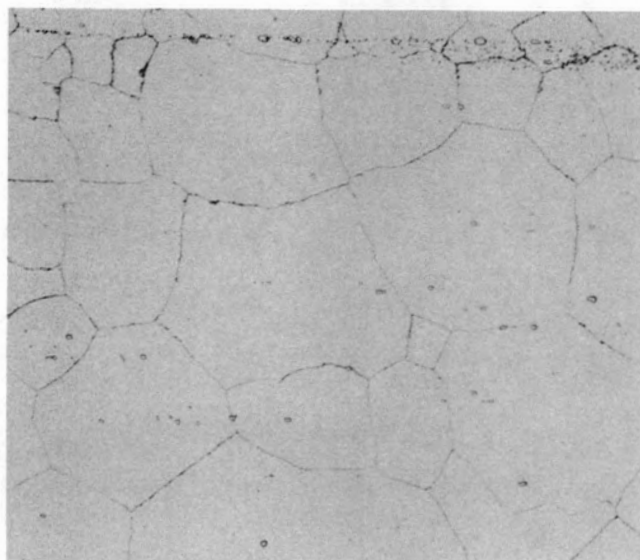
200  $\mu\text{m}$ 

Fig. A.5. Hastelloy X aged 20,000 h at 871°C.

ORNL-Photo 5588-81



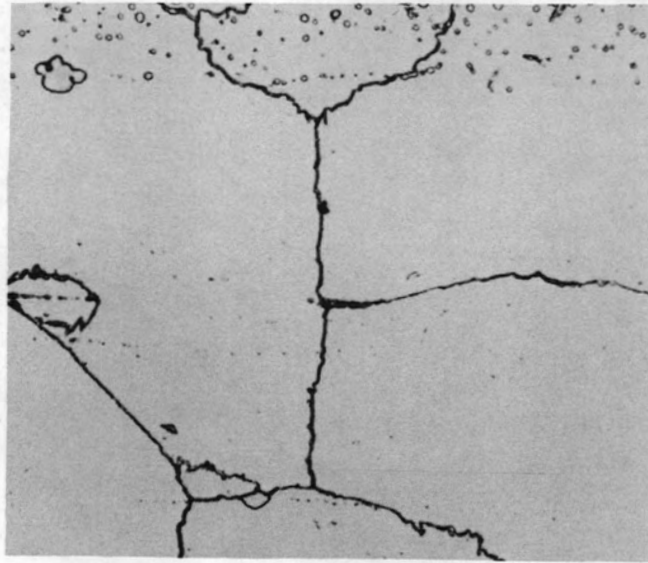
(a)

40  $\mu\text{m}$ 

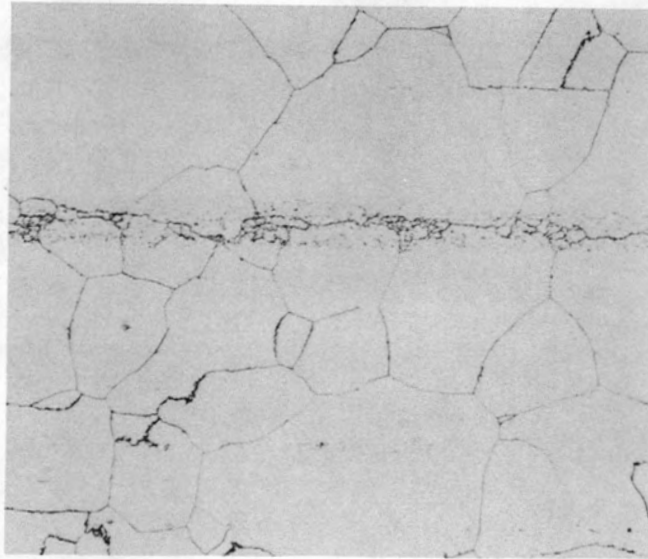
(b)

200  $\mu\text{m}$ 

Fig. A.6. Inconel 617 in solution-annealed condition.



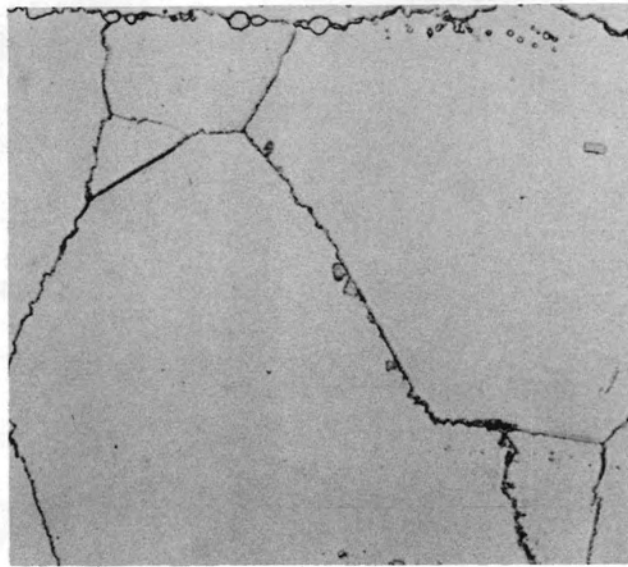
(a)

40  $\mu\text{m}$ 

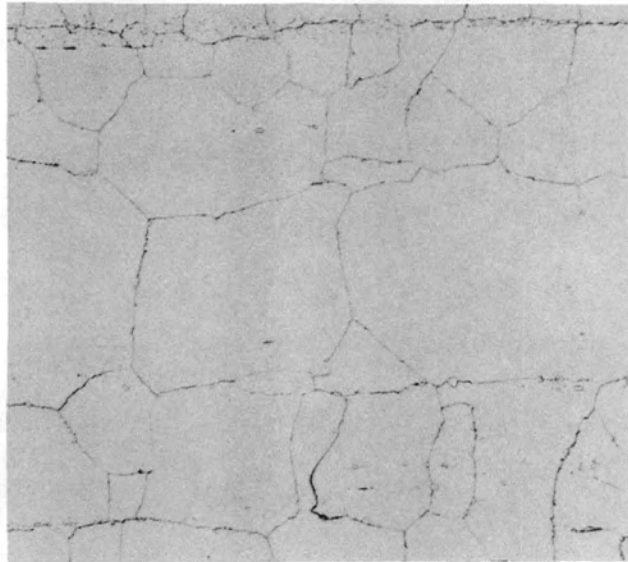
(b)

200  $\mu\text{m}$ 

Fig. A.7. Inconel 617 aged 10,000 h at 538°C.



(a)

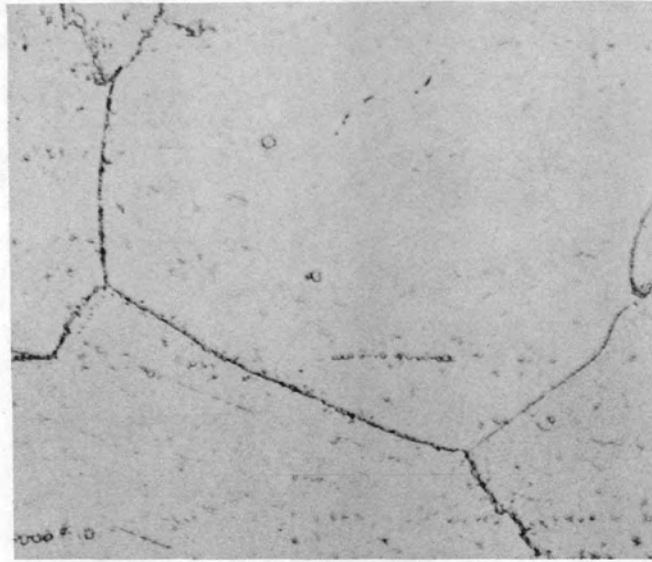
40  $\mu\text{m}$ 

(b)

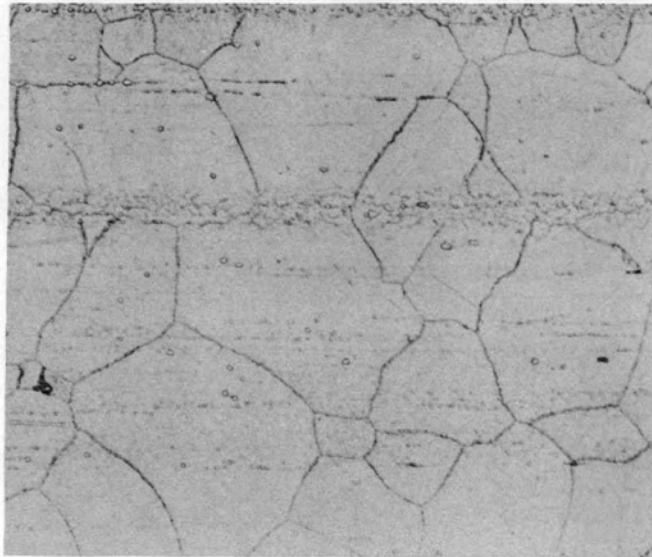
200  $\mu\text{m}$ 

Fig. A.8. Inconel 617 aged 20,000 h at 538°C.

ORNL-Photo 5591-81



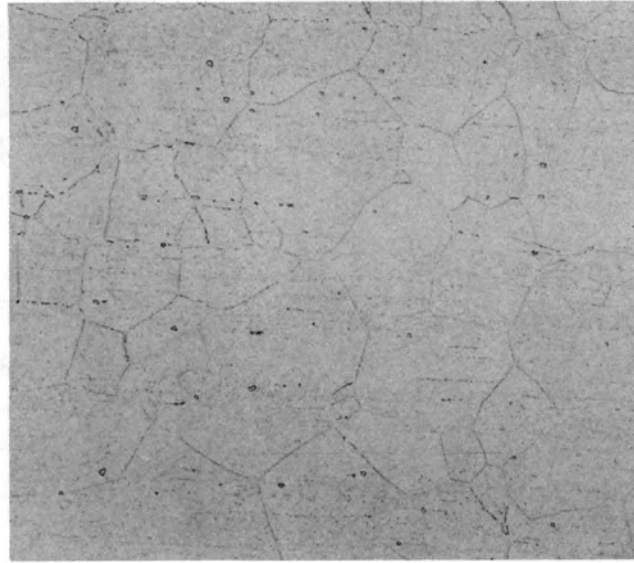
(a)

40  $\mu\text{m}$ 

(b)

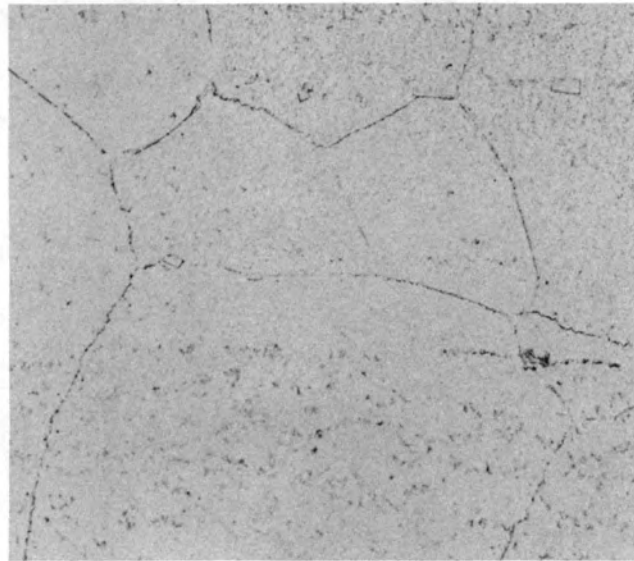
200  $\mu\text{m}$ 

Fig. A.9. Inconel 617 aged 10,000 h at 704°C.



(a)

200  $\mu\text{m}$

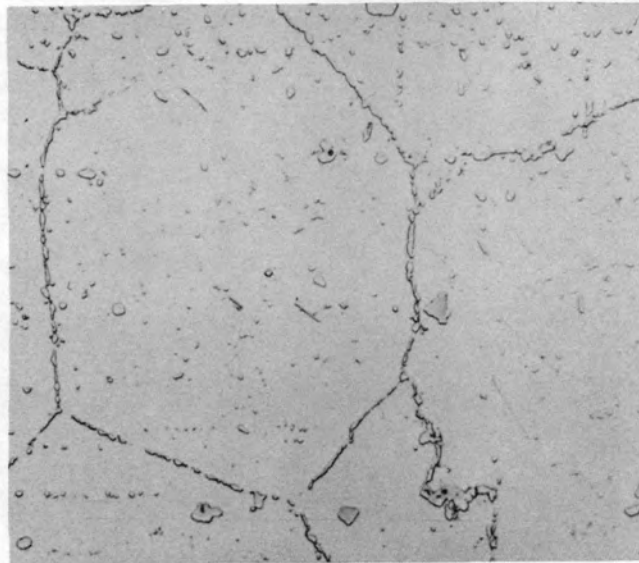


(b)

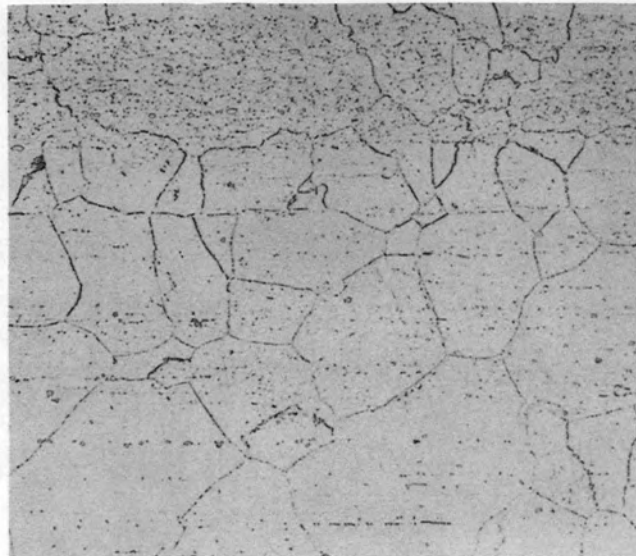
40  $\mu\text{m}$

Fig. A.10. Inconel 617 aged 20,000 h at 704°C.

ORNL-Photo 5593-81



(a)

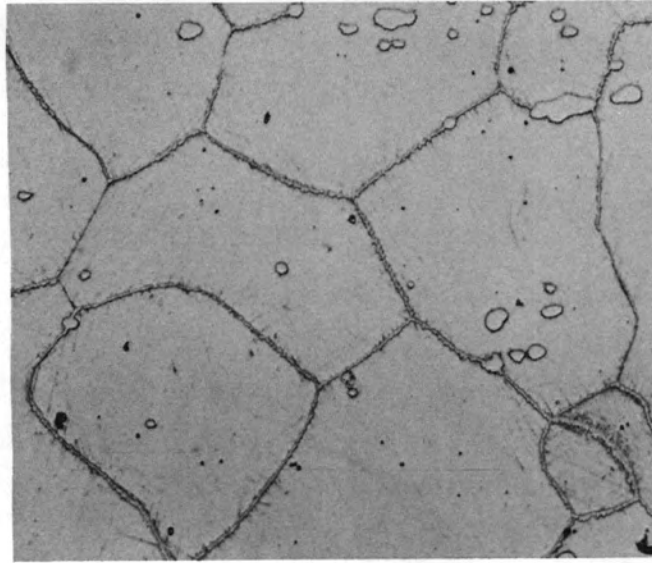
40  $\mu\text{m}$ 

(b)

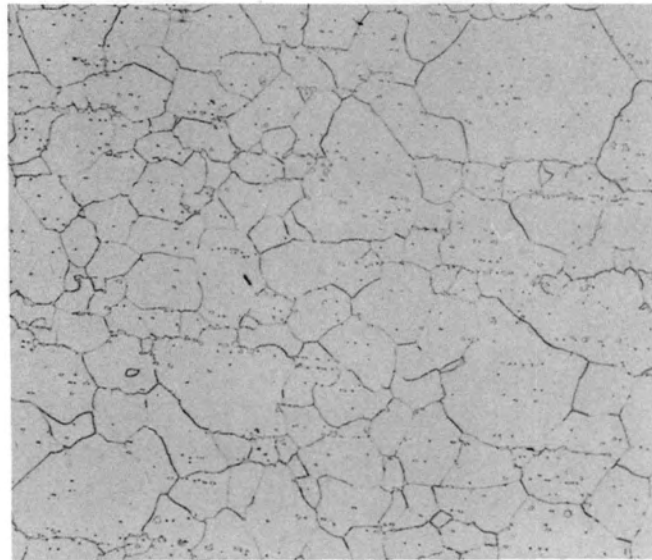
200  $\mu\text{m}$ 

Fig. A.11. Inconel 617 aged 10,000 h at 871°C.

ORNL-Photo 5594-81



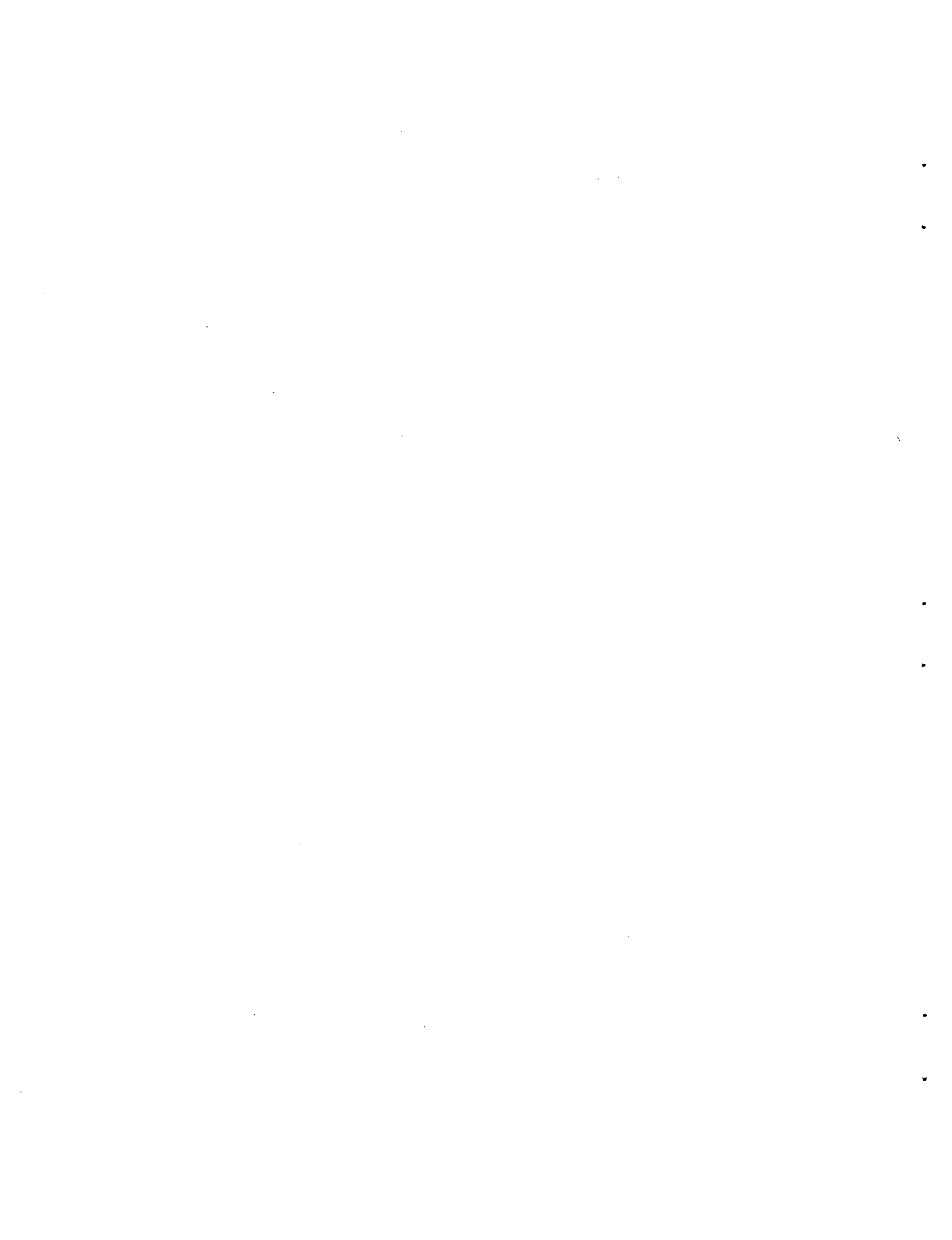
(a)

40  $\mu\text{m}$ 

(b)

200  $\mu\text{m}$ 

Fig. A.12. Inconel 617 aged 20,000 h at 871°C.



## Appendix B

## FATIGUE DATA

Included in Appendix B are fatigue data compilations for the following alloys tested in either air or impure helium: Inconel 617, Hastelloy C-4, Hastelloy X, Hastelloy C-176, and Hastelloy G.

Table B.1. Comparison of the nominal chemical composition of Hastelloy alloys for which fatigue data are reported

Element	Chemical composition, %			
	Hastelloy G	Hastelloy X	Hastelloy C-276	Hastelloy C-4
Ni	Bal	Bal	Bal	Bal
Co	2.50	0.50-2.50	2.5	2.0
Cr	21.0-23.5	20.5-23.0	14.50-16.50	14.00-18.00
Mo	5.50-7.50	8.0-10.0	15.00-17.00	14.00-17.00
W	1.00	0.20-1.00	3.00-4.50	
Fe	18.0	17.00-20.00	4.00-7.00	3.00
C	0.05	0.05-0.15	0.02	0.015
Si	1.00	1.00	0.08	0.08
Mn	1.0-2.0	1.00	1.00	1.00
Cu	1.50-2.50			
B		0.01		
Nb + Ta	1.75-2.50			
P	0.04	0.04	0.04	0.04
S	0.03	0.03	0.03	0.03
V			0.35	
Ti				0.70

Table B.2. Results of strain-controlled fatigue tests<sup>a</sup> on Hastelloy X (heat 2600-3-4936) generated in air

Specimen	Total strain range, $\Delta\epsilon_t$ (%)	Stress range, $\Delta\sigma$ (MPa)	Stress amplitude, MPa		Strain range, %		Cycles to failure, $N_f$
			Tensile $\sigma_t$	Compressive $\sigma_c$	Elastic $\Delta\epsilon_e$	Plastic $\Delta\epsilon_p$	
Solution-annealed material tested at 22°C							
HXL51	4.10	1,425	698	727	0.27	3.83	439
HXL29	3.04	1,392	681	711	0.70	2.34	591
HXL28	2.11	1,177	584	593	0.59	1.51	1,494
HXL27	1.50	968	478	490	0.49	1.02	6,101
HXL23	0.99	862	429	435	0.43	0.56	10,245
HXL47	0.89	829	407	422	0.42	0.47	15,796
HXL22	0.80	837	406	431	0.42	0.38	49,664
Solution-annealed material tested at 538°C							
HXL46	4.06	1,530	748	782	0.94	3.12	177
HXL16	3.02	1,353	665	688	0.83	2.19	418
HXL20	1.56	1,141	562	579	0.70	0.86	1,181
HXL30	0.99	1,015	494	521	0.63	0.36	5,182
HXL3	0.79	1,084	493	591	0.67	0.12	7,596
HXT2	0.71	855	405	450	0.53	0.18	14,240
HXT4	0.65	917	446	471	0.56	0.08	13,675
HXL19	0.60	877	444	433	0.54	0.06	225,000
Material aged 10,000 h at 538°C <sup>b</sup>							
X1203	3.55	1,476	731	745	0.91	2.64	111
X1209	1.89	1,128	552	576	0.70	1.11	753
X1206	0.92	979	483	496	0.60	0.32	1,632
X1207	0.83	824	407	417	0.51	0.32	4,150
X1208	0.74	866	421	445	0.53	0.21	5,226
X1205	0.68	821	400	421	0.51	0.17	11,784
X1210	0.56	720	355	365	0.44	0.12	11,713
Material aged 20,000 h at 538°C <sup>b</sup>							
X1304	1.87	1324	662	662	0.73	1.14	830
X1303	0.98	969	479	490	0.60	0.38	3,380
X1302	0.61	739	367	372	0.46	0.15	19,025
X1305	0.49	700	352	348	0.43	0.06	27,333
Solution-annealed material tested at 871°C							
HXL41	4.00	720	347	373	0.53	3.58	96
HXL40	3.01	715	343	372	0.52	2.49	138
HXL33	2.01	610	298	312	0.44	1.57	312
HXT7	1.50	604	297	266	0.38	1.06	466
HXL36	1.00	523	257	266	0.38	0.62	1,156
HXL43	0.80	479	236	243	0.35	0.45	2,002
HXL21	0.59	452	229	223	0.33	0.25	3,433
HXT6	0.50	392	195	197	0.28	0.22	13,234
Material aged 10,000 h at 871°C <sup>b</sup>							
X3204	3.71	700	350	350	0.52	3.19	106
X3207	2.22	689	341	348	0.50	1.72	170
X3203	1.71	672	332	340	0.49	1.22	255
X3202	1.14	569	286	283	0.42	0.72	624
X3205	0.70	480	240	240	0.35	0.35	1,950
X3201	0.58	449	228	221	0.33	0.25	2,991
X3206	0.41	399	202	197	0.29	0.12	11,570
Material aged 20,000 h at 871°C <sup>b</sup>							
X3304	2.75	638	321	317	0.47	2.28	162
X3303	1.86	599	303	296	0.44	1.42	333
X3302	0.97	521	259	262	0.38	0.59	1,044
X3301	0.60	448	233	215	0.32	0.28	4,854

<sup>a</sup>Fully reversed, continuous-cycling tests conducted at a strain rate of  $4 \times 10^{-3}$ /s, using a triangular waveform.

<sup>b</sup>Aged in argon; tested at the aging temperature.

Table B.3. Results of strain-controlled fatigue tests<sup>a</sup> on Hastelloy X (heat 2600-3-4936) generated in impure helium

Specimen	Total strain range, $\Delta\epsilon_t$ (%)	Stress range, $\Delta\sigma$ (MPa)	Stress amplitude, MPa		Strain range, %		Cycles to failure, $N_f$
			Tensile $\sigma_t$	Compressive $\sigma_c$	Elastic $\Delta\epsilon_e$	Plastic $\Delta\epsilon_p$	
Solution-annealed material tested at 538°C							
HXL93	2.74	725	355	370	0.45	2.29	378
HXL86	1.85	1,289	634	655	0.79	1.06	861
HXL85	0.96	993	490	503	0.61	0.35	4,277
HXL73	0.63	917	462	455	0.56	0.07	65,797
HXL94	0.49	755	255	500	0.46	0.03	1,978,430
Material aged 20,000 h at 538°C <sup>b</sup>							
X1308	0.95	877	427	450	0.52	0.33	3,000
X1306	0.60	820	386	434	0.51	0.09	60,774
Solution-annealed material tested at 871°C							
HX03	1.92	597	285	312	0.44	1.48	503
HX04	1.49	579	286	293	0.42	1.07	510
HX02	0.95	514	262	252	0.38	0.57	2,608
HXL95	0.50	496	243	253	0.36	0.14	9,886
HX01	0.50	459	231	228	0.34	0.16	8,124
Material aged 10,000 h at 871°C <sup>c</sup>							
X143	0.50	474	224	250	0.35	0.15	12,491

<sup>a</sup>Fully reversed, continuous-cycling tests conducted at a strain rate of  $4 \times 10^{-3}$ /s, using a triangular waveform.

<sup>b</sup>Aged in argon; tested at the aging temperature.

<sup>c</sup>Aged in impure helium; tested at the aging temperature.

Table B.4. Results of strain-controlled fatigue tests<sup>a</sup> on Inconel 617 (heat XX01A3U5 13-mm plate) generated in air

Specimen	Total strain range, $\Delta\epsilon_t$ (%)	Stress range, $\Delta\sigma$ (MPa)	Stress amplitude, MPa		Strain range, %		Cycles to failure, $N_f$
			Tensile $\sigma_t$	Compressive $\sigma_c$	Elastic $\Delta\epsilon_e$	Plastic $\Delta\epsilon_p$	
Solution-annealed material tested at 538°C							
IN24	3.60	1,472	741	731	0.83	2.77	60
IN23	2.73	1,413	689	724	0.79	1.94	181
IN19	1.93	1,296	641	655	0.73	1.20	316
IN47	1.42	1,261	627	634	0.71	0.71	498
IN20	1.07	1,057	514	543	0.59	0.48	2,357
IN22	1.00	948	465	483	0.53	0.47	2,009
IN21	0.69	906	441	465	0.51	0.18	4,672
IN18	0.52	834	400	434	0.47	0.05	11,520
IN25	0.50	663	315	348	0.37	0.13	10,929
IN53	0.43	766	383	383	0.41	0.02	41,180
Material aged 10,000 h at 538°C <sup>b</sup>							
I1201	1.85	1,254	627	627	0.71	1.14	432
I1205	1.40	1,310	641	669	0.74	0.66	610
I1202	0.94	990	483	507	0.56	0.38	2,575
I1206	0.56	865	403	462	0.49	0.07	20,116
I1203	0.50	751	372	379	0.42	0.08	17,105
I1204	0.40	672	334	338	0.38	0.02	23,166
Material aged 20,000 h at 538°C <sup>b</sup>							
I1304	1.84	1,324	662	662	0.74	1.10	715
I1301	0.94	1,055	510	545	0.59	0.34	3,796
I1305	0.68	907	445	462	0.51	0.17	10,352
Solution-annealed material tested at 704°C							
IN45	3.64	1,372	676	696	0.83	2.81	63
IN44	2.81	1,324	669	655	0.80	2.01	116
IN26	1.74	1,172	576	596	0.70	1.04	218
IN43	1.47	1,130	558	572	0.69	0.78	441
IN27	0.88	962	462	500	0.58	0.30	886
IN30	0.66	952	452	500	0.54	0.12	2,600
IN29	0.50	742	371	371	0.45	0.05	15,142
Material aged 10,000 h at 704°C <sup>b</sup>							
I2201	1.89	1,172	576	596	0.71	1.18	204
I2205	1.46	1,186	593	593	0.72	0.74	255
I2202	0.98	992	496	496	0.60	0.38	870
I2206	0.68	838	424	414	0.51	0.17	3,050
I2203	0.50	704	345	359	0.43	0.07	4,425
I2204	0.43	772	386	386	0.37	0.06	6,713

Table B.4. Continued

Specimen	Total strain range, $\Delta\epsilon_t$ (%)	Stress range, $\Delta\sigma$ (MPa)	Stress amplitude, MPa		Strain range, %		Cycles to failure, $N_f$
			Tensile $\sigma_t$	Compressive $\sigma_c$	Elastic $\Delta\epsilon_e$	Plastic $\Delta\epsilon_p$	
Material aged 20,000 h at 704°C <sup>b</sup>							
I2303	1.87	1,193	600	593	0.72	1.15	267
I2306	1.40	1,100	541	558	0.67	0.73	496
I2305	0.97	979	486	493	0.59	0.38	1,185
I2304	0.49	714	338	376	0.43	0.06	16,830
I2308	0.48	698	343	355	0.42	0.06	14,361
I2307	0.44	631	314	317	0.38	0.06	68,090
Solution-annealed material tested at 871°C							
IN42	3.62	734	365	369	0.49	3.13	75
IN41	2.76	748	369	379	0.50	2.26	135
IN38	1.80	686	334	352	0.45	1.35	207
IN40	1.42	686	341	345	0.45	0.97	370
IN35	0.92	579	283	296	0.38	0.54	753
IN39	0.81	583	293	290	0.39	0.42	935
IN36	0.67	564	276	288	0.37	0.30	1,216
IN37	0.60	529	265	264	0.35	0.25	1,608
IN32	0.51	480	221	259	0.32	0.19	2,304
IN34	0.42	491	238	253	0.32	0.10	2,715
IN33	0.42	459	219	240	0.30	0.12	5,700
Material aged 10,000 h at 871°C <sup>b</sup>							
I3201	1.89	710	355	355	0.47	1.42	219
I3205	1.45	734	369	365	0.49	0.96	209
I3202	0.97	589	293	296	0.39	0.58	526
I3206	0.58	512	260	252	0.33	0.25	2,182
I3203	0.50	535	271	264	0.35	0.15	1,232
I3204	0.41	493	245	248	0.33	0.07	1,385
Material aged 20,000 h at 871°C <sup>b</sup>							
I3303	1.87	659	331	328	0.44	1.43	215
I3301	0.92	562	279	283	0.37	0.55	775
I3302	0.50	473	240	233	0.31	0.19	2,231
I3304	0.41	455	236	219	0.30	0.11	3,087

<sup>a</sup>Fully reversed, continuous-cycling tests conducted at a strain rate of  $4 \times 10^{-3}$ /s, using a triangular waveform.

<sup>b</sup>Aged in argon; tested at the aging temperature.

Table B.5. Results of strain-controlled fatigue tests<sup>a</sup> on Inconel 617 (heat XX01A3U5) generated in impure helium

Specimen	Total strain range, $\Delta\epsilon_t$ (%)	Stress range, $\Delta\sigma$ (MPa)	Stress amplitude, MPa		Strain range, %		Cycles to failure, $N_f$
			Tensile $\sigma_t$	Compressive $\sigma_c$	Elastic $\Delta\epsilon_e$	Plastic $\Delta\epsilon_p$	
Solution-annealed material tested at 538°C							
IN57	1.86	1,372	689	683	0.77	1.09	990
IN49	0.96	1,168	572	596	0.66	0.30	6,680
IN60	0.55	979	462	517	0.54	0.01	383,580
Material aged 20,000 h at 538°C <sup>b</sup>							
I1306	1.00	1,146	555	591	0.64	0.36	8,760
I1307	0.58	961	403	558	0.54	0.04	143,109
Solution-annealed material tested at 704°C							
IN52	1.81	1,358	662	696	0.82	0.99	400
IN54	0.87	1,100	521	579	0.67	0.20	2,531
IN55	0.55	827	410	417	0.50	0.05	30,879
IN50	0.54	838	436	402	0.51	0.03	89,404
Material aged 20,000 h at 704°C <sup>b</sup>							
I2310	0.86	1,024	493	531	0.62	0.24	2,825
I2309	0.55	810	369	441	0.49	0.06	31,359
Solution-annealed material tested at 871°C							
IN61	1.60	564	285	279	0.37	1.23	661
IN62	1.00	571	290	281	0.38	0.62	1,097
IN63	0.50	556	265	291	0.37	0.13	9,152
Material aged 20,000 h at 871°C <sup>b</sup>							
I3306	0.48	444	222	222	0.28	0.20	5,865

<sup>a</sup>Fully reversed, continuous-cycling tests conducted at a strain rate of  $4 \times 10^{-3}$ /s, using a triangular waveform.

<sup>b</sup>Aged in argon; tested at the aging temperature.

Table B.6. Interatom data<sup>a</sup>


---

Base material, 22.2-mm-diam bar

Grain size, ASTM 2.5

Yield strength, MPa

Room temperature	333
850°C	196

Ultimate tensile strength, MPa

Room temperature	760
850°C	256

Cycles to failure

$\Delta\epsilon_t = 0.3\%$	14,280; 9,726
$\Delta\epsilon_t = 0.6\%$	1,364; 1,566
$\Delta\epsilon_t = 1.0\%$	450; 494
$\Delta\epsilon_t = 1.5\%$	286; 267

Parameters of  $AN_f^{-a} + BN_f^{-b}$

$A$	0.009
$a$	0.1275
$B$	1.9951
$b$	0.9352

---

<sup>a</sup>Data generated at 850°C in air on Hastelloy X.

Source of data: E. D. Grosser, Interatom, Abt, 8320, Postfach, D-5060, Bensburg, Federal Republic of Germany. Additional information may be found in H. P. Meurer, H. Breitling, and E. D. Grosser, "Fatigue and Creep-Fatigue Behavior of High-Temperature Alloys for HTR-Application," pp. U-1-U-12 in *Proceedings of IAEA Specialists' Meeting on High Temperature Metallic Materials for Application in Gas Cooled Reactors, Vienna, May 4-6, 1981*, IAEA, Vienna, 1981.

Table B.7. Low-cycle fatigue data<sup>a</sup> for Hastelloy C-276 (heat 2760-1-3299) tested in air in computed axial strain control,  $A = \infty$

Specimen	Total strain range, $\Delta\epsilon_t$ (%)	Stress range, $\Delta\sigma$ (MPa)	Stress amplitude, MPa		Strain range, %		Cycles to failure, $N_f$
			Tensile $\sigma_t$	Compressive $\sigma_c$	Elastic $\Delta\epsilon_e$	Plastic $\Delta\epsilon_p$	
Tested at room temperature, Young's modulus $E = 141$ GPa							
C2A-1	1.0	776	496	479	0.475	0.525	15,768
C2A-2	4.0	1,544	758	786	0.752	3.284	871
C2A-3	0.7	903	462	441	0.44	0.26	32,654
C2A-4	2.8	1,334	662	672	0.65	2.15	1,728
C2A-5	1.3	1,034	517	517	0.504	0.796	9,086
C2A-6	2.0	1,179	590	589	0.573	1.427	4,173
Tested at 427°C, Young's modulus $E = 126$ GPa							
C2A-13	1.0	1,034	510	524	0.57	0.43	4,908
C2A-14	4.0	1,620	779	841	0.89	3.11	398
C2A-15	0.52	786	393	393	0.43	0.09	30,413
C2A-16	0.65	886	437	449	0.486	0.164	16,784

<sup>a</sup>Data generated at a strain rate of  $5 \times 10^{-3}$ /s in uniaxial push-pull fatigue by Mar-Test Inc. An hourglass-shaped specimen geometry was employed with a 6.35-mm-gage (0.25 in.) diameter. Heat 2760-1-3299 tested in the mill-annealed condition with an ASTM grain size of 4 (78  $\mu\text{m}$ ). Longitudinal axis of specimen perpendicular to the rolling direction. Courtesy of Cabot Corp., Kokomo, Ind.

Table B.8. Fatigue data<sup>a</sup> for Hastelloy C-276 tested in air (3/4-in. plate; heat 2760-0-3172; grain size ASTM 3-4)

Specimen	Total strain range, $\Delta\epsilon_t$ (%)	Stress range, $\Delta\sigma$ (MPa)	Stress amplitude, MPa		Strain range, %		Cycles to failure, $N_f$
			Tensile $\sigma_t$	Compressive $\sigma_c$	Elastic $\Delta\epsilon_e$	Plastic $\Delta\epsilon_p$	
Tests conducted at room temperature							
90-81	2.98	1,345	661	684	0.66	2.32	786
88-81	1.96	1,177	581	596	0.57	1.39	2,632
89-81	1.48	1,085	538	546	0.53	0.95	5,358
85-81	0.69	914	450	464	0.44	0.25	27,497
91-81	0.6	897	441	456	0.44	0.16	48,757
86-81	0.49	844	422	422	0.41	0.08	139,910
92-81 <sup>b</sup>	0.4	785	385	400	0.38	0.02	368,350
93-81 <sup>c</sup>	0.346	779	351	428	0.34	0.006	>1,300,000
Tests conducted at 482°C							
118-81 <sup>d</sup>	1.5						1,845
113-81	0.45	868	440	428	0.0	0.0	262,465

<sup>a</sup>Axial strain control fully reversed triangular waveform with a strain rate of  $5 \times 10^{-3}$ /s, using a uniform-gage specimen 6.35 mm (0.25 in.) in diameter and 19.05 mm (0.75 in.) long. Material tested at Cabot Corp. in mill-annealed condition with longitudinal axis of specimen perpendicular to the rolling direction of the plate. Courtesy of Cabot Corp., Kokomo, Ind.

<sup>b</sup>Switched to load control mode after 50,000 cycles and continued at a frequency of 10 Hz.

<sup>c</sup>Switched to load control mode after 17,000 cycles and continued at a frequency of 10 Hz; specimen did not break; tests discontinued.

<sup>d</sup>Switched to load control mode after 186,000 cycles and continued at a frequency of 10 Hz; specimen broke in shoulder.

Table B.9. Fatigue data<sup>a</sup> at room temperature for Hastelloy C-276 tested in air (3/4-in. plate; heat 2760-0-3171; grain size ASTM 4-4.5)

Specimen	Total strain range, $\Delta\epsilon_t$ (%)	Stress range, $\Delta\sigma$ (MPa)	Stress amplitude, MPa		Strain range, %		Cycles to failure, $N_f$
			Tensile $\sigma_t$	Compressive $\sigma_c$	Elastic $\Delta\epsilon_e$	Plastic $\Delta\epsilon_p$	
98-81	3.0	1,372	675	697	0.67	2.33	633
97-81	1.97	1,206	597	609	0.59	1.38	2,931
95-81	1.0	1,017	505	512	0.5	0.5	13,204
96-81 <sup>b</sup>	0.496	890	435	456	0.062	0.434	128,510
94-81 <sup>c</sup>	0.389	792	399	393	0.003	0.386	>2,500,000

<sup>a</sup>Axial strain control fully reversed triangular waveform with a strain rate of  $5 \times 10^{-3}$ /s generated by Cabot Corp. on uniform-gage specimens 6.35 mm (0.25 in.) in diameter and 19.05 mm (0.75 in.) long. Material tested in mill-annealed condition with longitudinal axis of specimen perpendicular to the rolling direction of plate. Courtesy of Cabot Corp., Kokomo, Ind.

<sup>b</sup>Switched to load control mode and continued the test at 2.5 Hz.

<sup>c</sup>Switched to load control mode and continued the test at 10 Hz; specimen did not break; test discontinued.

Table B.10. Low-cycle fatigue data<sup>a</sup> for Hastelloy alloy G tested in air in computed axial strain control ( $A = \infty$ )

Specimen	Total strain range, $\Delta\epsilon_t$ (%)	Stress range, $\Delta\sigma$ (MPa)	Stress amplitude, MPa		Strain range, %		Cycles to failure, $N_f$
			Tensile $\sigma_t$	Compressive $\sigma_c$	Elastic $\Delta\epsilon_e$	Plastic $\Delta\epsilon_p$	
Tested at room temperature, Young's modulus $E = 132$ GPa							
GA-1	2.5	1,234	617	617	0.64	1.88	1,289
GA-2	0.9	868	434	434	0.454	0.46	14,580
GA-3	0.6	786	393	393	0.41	0.20	46,395
GA-4	1.5	1,003	496	507	0.523	0.98	4,129
GA-5	4.0	1,489	724	765	0.78	3.12	396
Tested at 427°C, Young's modulus $E = 116$ GPa							
GA-6	4.0	1,489	738	751	0.89	3.04	223
GA-7	1.4	1,054	527	527	0.632	0.76	2,465
GA-8	0.6	862	441	441	0.516	0.068	26,240

<sup>a</sup>Fully reversed axial strain controlled data with a strain rate of  $5 \times 10^{-3}$ /s obtained by Mar-Test Inc. Hourglass-shaped specimens with a 6.35-mm diameter were employed. Material came from 25.4-mm-diam (1.0-in.) bar, heat 1880-8-5942, with a grain size of ASTM 2.5-3. Courtesy of Cabot Corp., Kokomo, Ind.

Table B.11. Fatigue data<sup>a</sup> at room temperature for Hastelloy alloy G tested in air (3/4-in. plate; heat 2340-0-2508)

Specimen	Total strain range, $\Delta\epsilon_t$ (%)	Stress range, $\Delta\sigma$ (MPa)	Stress amplitude, MPa		Strain range, %		Cycles to failure, $N_f$
			Tensile $\sigma_t$	Compressive $\sigma_c$	Elastic $\Delta\epsilon_e$	Plastic $\Delta\epsilon_p$	
103-81	2.0	1,080	530	550	0.56	1.44	2,065
102-81	0.99	886	439	447	0.46	0.53	12,460
101-81	0.7	803	396	407	0.42	0.28	35,342
105-81	0.55	768	372	396	0.4	0.15	95,791
99-81 <sup>b</sup>	0.5	760	370	390	0.4	0.1	133,003
106-81 <sup>c</sup>	0.45	722	354	368	0.38	0.07	266,100
100-81 <sup>d</sup>	0.395	691	332	359	0.36	0.035	>1,700,000

<sup>a</sup>Axial strain control with fully reversed loading at a strain rate of  $5 \times 10^{-3}$ /s. Data generated by the Cabot Corp., using uniform-gage specimens with a 6.35-mm (0.25-in.) gage diameter and 19.05 mm (0.75 in.) long. Material had an ASTM grain size of 3.5-4.0, and specimens were fabricated with longitudinal axis of specimen perpendicular to the rolling direction. Courtesy of Cabot Corp., Kokomo, Ind.

<sup>b</sup>Switched to load control mode after 50,000 cycles and continued the test at 2.5 Hz.

<sup>c</sup>Switched to load control mode after 47,000 cycles and continued the test.

<sup>d</sup>Switched to load control mode after 12,000 cycles and continued the test at 10 Hz; specimen did not fail; test was discontinued.

Table B.12. Room-temperature strain-controlled fatigue data<sup>a</sup> for Hastelloy C-4 tested in air at a strain rate of  $5 \times 10^{-3}$ /s under fully reversed triangular strain waveform ( $A_{\epsilon} = \infty$ )

Specimen	Total strain range, $\Delta\epsilon_t$ (%)	Stress range, $\Delta\sigma$ (MPa)	Stress amplitude, MPa		Strain range, %		Cycles to failure, $N_f$
			Tensile $\sigma_t$	Compressive $\sigma_c$	Elastic $\Delta\epsilon_e$	Plastic $\Delta\epsilon_p$	
Heat 0-0946 <sup>b</sup>							
138-81	2.0	1,242	614	628	0.58	1.42	2,403
134-81	1.5	1,157	573	584	0.54	0.96	5,246
135-81	1.0	1,047	521	526	0.49	0.51	12,364
136-81	0.55	908	445	463	0.43	0.12	86,839
137-81	0.51	885	441	445	0.42	0.09	136,358
139-81	0.45	871	429	441	0.41	0.04	693,096 <sup>c</sup>
143-81	0.4	824	394	430	0.383	0.017	1,450,000 <sup>d,e</sup>
Heat 0-0920 <sup>f</sup>							
145-81	2.0	1,223	598	625	0.58	1.42	2,394
146-81	1.0	1,033	505	528	0.47	0.53	10,400
144-81	0.6	896	444	452	0.42	0.18	57,677
148-81	0.5	865	424	441	0.41	0.09	161,700
Heat unknown <sup>g</sup>							
	0.4	776	381	395	0.37	0.03	1,180,000 <sup>d,e</sup>
4	3.0	1,427	646	731	0.67	2.33	1,417
1	1.0	1,058	525	533	0.5	0.5	12,363
2	0.8	973	483	440	0.458	0.342	23,048
3	0.7	965	483	483	0.455	0.245	38,794

<sup>a</sup>Data furnished by courtesy of Cabot Corp., Kokomo, Ind.

<sup>b</sup>Plate, 12.7 mm; grain size, ASTM 5-5.5; tests conducted by Cabot Corp.

<sup>c</sup>After about  $10^5$  cycles continued the test at 5 Hz in strain control mode.

<sup>d</sup>After about  $10^5$  cycles switched to load control mode and continued the test at 10 Hz.

<sup>e</sup>Specimen did not break; test discontinued.

<sup>f</sup>Bar, 19.0 mm; grain size, ASTM 5-5.5; tests conducted by Cabot Corp.

<sup>g</sup>Tests conducted by Mar-Test.

## Appendix C

## PROPOSED FATIGUE DESIGN CURVES

Available continuous cycling fatigue data for Hastelloy X (refs. 1 and 2) and the related Hastelloy alloys G (ref. 3), C-276 (ref. 3), and C-4 (ref. 4) were analyzed to establish a description of the fatigue behavior of these materials for use in developing fatigue design curves for Section III of the *ASME Boiler and Pressure Vessel Code*. Data were available at room temperature and at 427°C (800°F), with cycling lives ranging from less than 100 to more than  $10^7$  cycles. Preliminary analysis showed that all four of the above materials exhibited similar fatigue behavior, and it was judged appropriate to combine them into a single data base. It was then found possible to obtain acceptable fits to the combined data in terms of cyclic lives as a function of applied strain range by using a modification of the popular Langer equation.<sup>5</sup> These fitted curves were then transformed into the format of the ASME code fatigue design curves, using standard techniques.

## Choice of Data

Data used were taken from the compilations given in refs. 1 through 5. Most data were from strain-controlled tests. Data from load-controlled tests at room temperature were also used but only if the lives extended beyond  $10^6$  cycles. Thus, we were able to assume elastic behavior in these tests and to convert applied stress range to strain range simply by dividing by an elastic modulus of 195 GPa ( $28.3 \times 10^6$  psi). Runouts were generally excluded from the data base with the exception of two tests at the lowest available stress range, which lasted more than  $10^7$  cycles before termination. We felt that these two tests contributed significantly to the data base and included them in the analysis; the lives at which they were terminated were treated as the total cyclic lives for those tests. (More sophisticated and more accurate techniques<sup>6</sup> exist for estimation of the cyclic lives from runout tests, but we felt that it was not necessary to apply these techniques in this instance.) Otherwise, all

available data were initially used. The data of Jablonski<sup>7</sup> (Fig. 1), however, were later excluded because they showed significantly shorter lives than corresponding data from other sources.

#### Analysis Technique

Although the Langer equation is somewhat limited and inflexible for fitting experimental data, it is a popular one and has often been used in developing fatigue design curves for the ASME code. In its original form, the equation is

$$S = BN^{-1/2} + S_e , \quad (1)$$

where  $N$  is the cyclic life,  $S$  is a "pseudostress amplitude" given by  $1/2(\Delta\epsilon_t)E$ ,  $\Delta\epsilon_t$  being the total applied strain range and  $E$  the elastic modulus. The parameters  $B$  and  $S_e$  are optimized to obtain best fits to the available data, with  $S_e$  corresponding to an "endurance limit" or to the pseudostress amplitude, at and below which cyclic life becomes infinite.

Because most of the available data in refs. 1 through 4 were from strain-controlled tests, we decided to perform fits to the data directly in terms of strain range rather than pseudostress range. Equation (1) can easily be transformed to

$$\Delta\epsilon_t = B^*N^{1/2} + \Delta\epsilon_0 , \quad (2)$$

to accomplish this choice. However, Eq. (2) still suffers from extreme inflexibility and from the fact that it is written with strain range as the dependent variable even though, by nature of the fatigue test, life is the appropriate choice for the dependent variable. Therefore, we decided to make the exponent on life in Eq. (2) a variable to be optimized for best fit to the data and to solve the equation for life (or some transformation thereof) as the dependent variable. This step resulted in the equation

$$\log N = B_1 \log(\Delta\epsilon_t - \Delta\epsilon_0) + B_0 , \quad (3)$$

where  $B_0$ ,  $B_1$ , and  $\Delta\epsilon_0$  are constants to be optimized by fits to the data, with  $\Delta\epsilon_0$  corresponding to an endurance limit in terms of strain range. Equation 3 is nonlinear in the regression coefficients and therefore cannot be directly fit to data by using simple linear least squares regression. Our approach to this problem was to guess values for  $\Delta\epsilon_0$  (which allows  $B_0$  and  $B_1$  to be estimated by linear least squares) and to iteratively modify these guesses to obtain optimum fit to the data in terms of the variance of the fit. We also perform different transformations on the dependent variable in order to optimize the fits and to obtain approximately uniform variance over the entire range of cyclic lives examined. The equation finally chosen as giving optimum representation for fatigue behavior was

$$\log(\log N) = 0.560 - 0.190 \log(\Delta\epsilon_t - 0.34) . \quad (4)$$

Note that the  $\log(\log N)$  transformation was also found to be optimum in a recent survey of several hundred sets of fatigue data (~4600 separate tests) on a variety of materials.<sup>8</sup> Thus, a great deal of information supports the use of this transformation.

Figure C.1 illustrates the fit of Eq. (4) to available data [ $X = \log(\Delta\epsilon_t - 0.34)$ ,  $Y = \log(\log N)$ ], whereas Fig. C.2 shows a standard residual plot. One short-term low-cycle test appears possibly to have failed prematurely, but, in general, the fit is excellent, and the variance from the fit is uniform in cyclic life over the range of the data.

Figure C.3 compares available data with the predictions from Eq. (4) in a plot of a standard log strain range versus log cycles to failure. The fit to the data is quite good, although in the low-cycle fatigue region a consistent and systematic trend seems to show the fatigue life at 427°C to be less than that at room temperature. (This trend disappears by about  $10^5$  cycles, above which there are insufficient data to determine whether the trend is actually reversed at higher numbers of cycles.) Section III of the ASME code typically includes a single curve from room temperature to about 427°C, however, and our mean curve represents a good compromise between these two temperatures. It was therefore decided, with

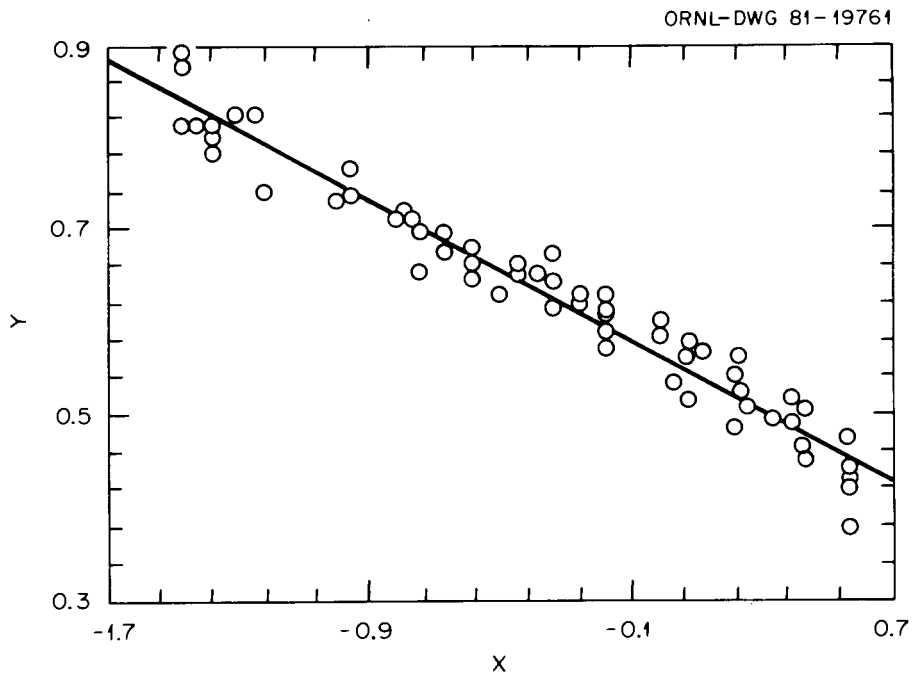


Fig. C.1. Comparison of best-fit line (dotted) with experimental data (points) in transformed units.  $Y = \log(\log N)$ ;  $X = \log(\Delta\epsilon_t - 0.34)$ .

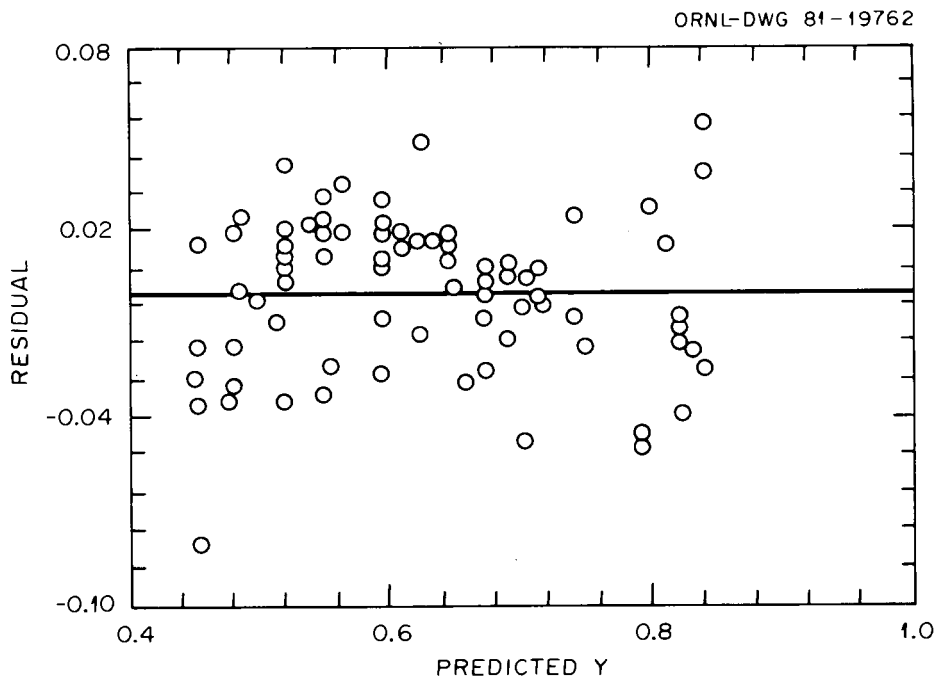


Fig. C.2. Residual plot for Hastelloy alloy fatigue data.  $Y = \log(\log N)$ ; residual = predicted—observed values of  $Y$ .

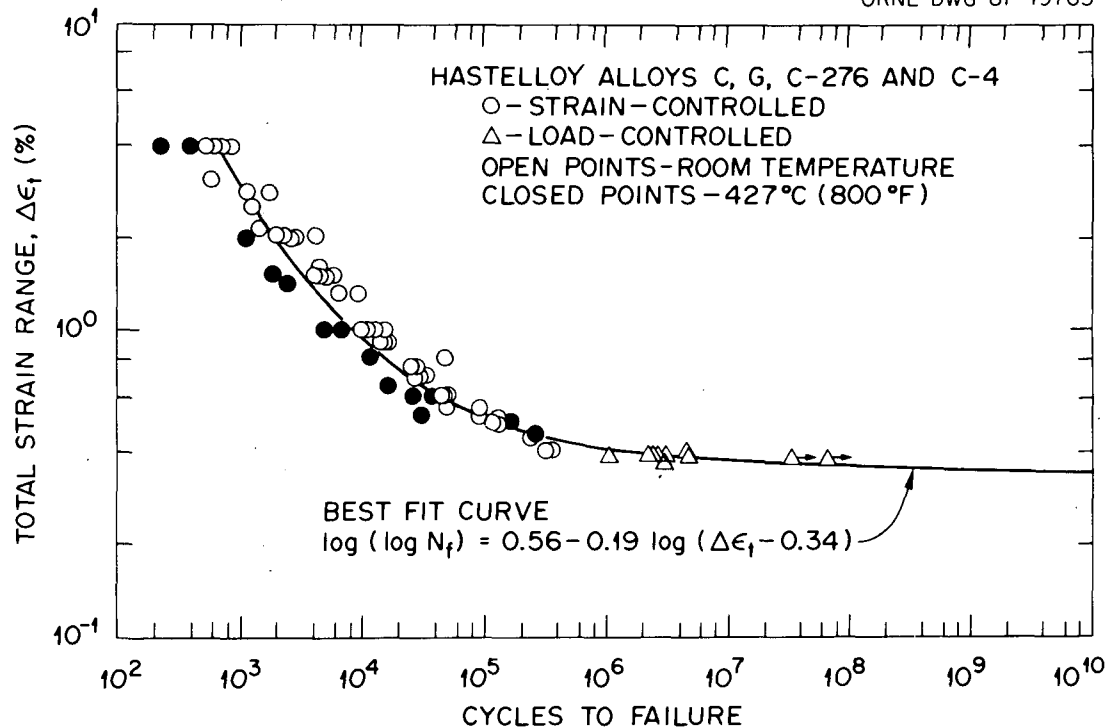


Fig. C.3. Comparison of predicted fatigue curve for Hastelloy alloys with experimental data.

concurrence of the ASME Subgroup on Fatigue Strength, to propose this single curve and to ignore the slight temperature dependence evidenced by the data shown in Fig. C.3.

The mean curve in Fig. C.3 can now be converted to a design curve by applying a standard ASME design factor of the more conservative of "20 on cycles" or "2 on strain range." This curve can then be transformed to normal units of pseudostress amplitude by multiplying the strain range values by  $E/2$ . We performed this transformation by assuming a modulus  $E$  of 195 GPa ( $28.3 \times 10^6$  psi). The resultant curve is then in standard ASME Section III format, with the exception of a correction for mean stress effects.

#### Mean Stress Effects

No data were available on the effects of mean stress on the fatigue behavior of the Hastelloy alloys examined in this study. We therefore

applied the commonly used<sup>9</sup> Goodman correction for maximum effects of mean stress. This approach relates the corrected pseudostress amplitude  $S'$  to the uncorrected amplitude  $S$  by

$$S' = S (S_u - S_y) / S_u + S_y , \quad (5)$$

where  $S_u$  is the ultimate tensile strength and  $S_y$  is the cyclic yield strength.

From data supplied in refs. 1 through 4, the ultimate tensile strength for these alloys is summarized in Table C.1. Although there is some variation among alloys, it seems reasonable to accept average values from the four alloys as representative, especially given the variations in properties often observed for various lots of material.

Figure C.4 summarizes the cyclic stress-strain properties of the current alloys in terms of stress amplitude versus strain amplitude at the half life of a fatigue test. The data seem to fall into two distinct bands. All data at 427°C and the room-temperature data for alloys C-276 and C-4 fall in the upper band; the room-temperature data for alloys X and G fall in the lower. Thus, for alloys X and G there is an apparent tendency toward development of higher cyclic stresses at 427°C than at room temperature. For alloy C-276, however, there is no apparent temperature dependence in cyclic stress-strain behavior. (Data for alloy C-4 were available only at room temperature.) An average room-temperature 0.2% offset  $S_y$  would be about 454 MPa (65.8 ksi), whereas the average 427°C

Table C.1. Average ultimate tensile strength values for Hastelloy alloys

	Ultimate tensile strength for Hastelloy alloy, MPa				
	X	C-276	G	C-4	Average
Room temperature	108	113	100	117	110
427°C (800°F)	100	92	82	100	94

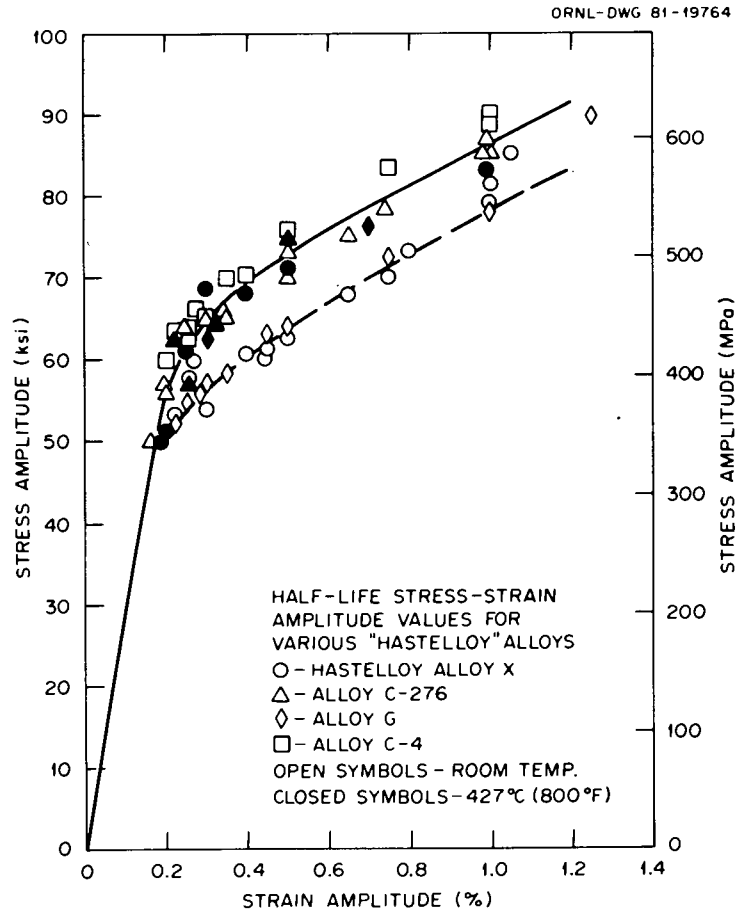


Fig. C.4. Cyclic stress-strain behavior of Hastelloy alloys.

would be about 490 MPa (71 ksi). However, an  $S_y$  value of 414 MPa (60 ksi) should be sufficient as an indicator of the onset of plastic strain at either temperature. Still, even if one uses this latter value for  $S_u$ , the higher ultimate tensile strength at room temperature leads to different mean stress correction factors for the two temperatures. Because mean stresses would commonly develop in thermal fatigue situations (temperature cycling from low to high), it would seem reasonable to adopt a compromise mean stress correction. Therefore, the correction factors used were obtained by averaging the room temperature and the 427°C correction factors for a given pseudostress amplitude.

Figure C.5 shows the final curve obtained in the above manner. This curve is recommended for use in both strain- and load-controlled situations (since no differences between the two were apparent) from room temperature to 427°C.

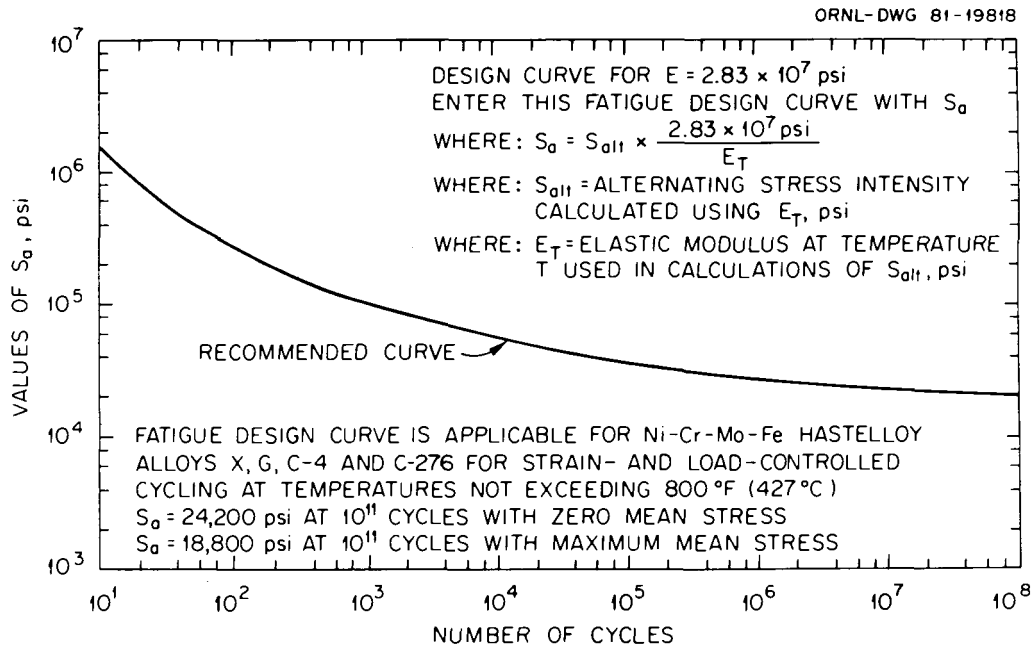


Fig. C.5. Design fatigue curve for Hastelloy alloys.

#### REFERENCES FOR APPENDIX C

1. A. Aizaz, *Fatigue Behavior of Hastelloy Alloy X*, T.F. 10204, Cabot Corporation, Kokomo, Ind., 1980.
2. A. Aizaz, *Fatigue Data on Hastelloy X*, T.F. 10488, Cabot Corporation, Kokomo, Ind., June 1981.
3. A. Aizaz, *Fatigue Behavior of Hastelloy Alloys C-276 and G*, T.F. 10498, Cabot Corporation, Kokomo, Ind., June 1981.
4. A. Aizaz, *Fatigue Behavior of Hastelloy Alloy C-4*, T.F. 10587, Cabot Corporation, Kokomo, Ind., Aug. 1981.
5. B. F. Langer, "Design of Pressure Vessels for Low-Cycle Fatigue," *J. Basic Eng.* 84(3): 389-402 (1962).
6. J. Schmee and G. J. Hahn, "A Simple Method for Regression Analysis with Censored Data," *Technometrics* 21(4): 417-32 (1979).
7. D. A. Jablonski, "Fatigue Behavior of Hastelloy X at Elevated Temperature in Air Vacuum and Oxygen Environments," Ph.D. thesis, Department of Material Science and Engineering, Massachusetts Institute of Technology, Cambridge, 1978.
8. D. T. Raske, Argonne National Laboratory, Argonne, Ill., personal communication to M. K. Booker, September 1981.

ORNL/TM-8130  
 Distribution  
 Category UC-77

## INTERNAL DISTRIBUTION

- |        |                               |        |                                  |
|--------|-------------------------------|--------|----------------------------------|
| 1-2.   | Central Research Library      | 39.    | C. J. Long, Jr.                  |
| 3.     | Document Reference Section    | 40.    | H. E. McCoy, Jr.                 |
| 4-5.   | Laboratory Records Department | 41.    | J. C. Ogle                       |
| 6.     | Laboratory Records, ORNL RC   | 42.    | A. R. Olsen                      |
| 7.     | E. J. Allen                   | 43-47. | P. L. Rittenhouse                |
| 8-12.  | M. K. Booker                  | 48.    | G. M. Slaughter                  |
| 13-17. | C. R. Brinkman                | 49.    | J. E. Smith                      |
| 18.    | C. W. Collins                 | 50-54. | J. P. Strizak                    |
| 19.    | Uri Gat                       | 55.    | F. W. Wiffen                     |
| 20.    | M. L. Grossbeck               | 56.    | M. H. Yoo                        |
| 21.    | J. P. Hammond                 | 57.    | A. L. Bement, Jr. (Consultant)   |
| 22-24. | M. R. Hill                    | 58.    | E. H. Kottcamp, Jr. (Consultant) |
| 25.    | J. A. Horak                   | 59.    | Alan Lawley (Consultant)         |
| 26.    | H. Inouye                     | 60.    | T. B. Massalski (Consultant)     |
| 27-36. | P. R. Kasten                  | 61.    | R. H. Redwine (Consultant)       |
| 37.    | J. F. King                    | 62.    | K. M. Zwilsky (Consultant)       |
| 38.    | E. H. Lee                     |        |                                  |

## EXTERNAL DISTRIBUTION

- 63-64. DOE, HIGH TEMPERATURE REACTOR PROGRAM, Washington, DC 20545  
 J. E. Fox  
 G. A. Newby
65. DOE, OFFICE OF NUCLEAR POWER SYSTEMS, Washington, DC 20545  
 Director
66. DOE, SAN-San Diego, 110 West A Street, Suite 460, San Diego,  
 CA 92101  
 Manager
67. DOE, OAK RIDGE OPERATIONS OFFICE, P.O. Box E, Oak Ridge, TN 37830  
 Office of Assistant Manager for Energy Research and Development
- 68-215. DOE, TECHNICAL INFORMATION CENTER, OFFICE OF INFORMATION SERVICES,  
 P.O. Box 62, Oak Ridge, TN 37830  
 For distribution as shown in TID-4500 Distribution Category,  
 UC-77 (Gas Cooled Reactor Technology)